The Plant Cell, Vol. 24: 3106–3118, July 2012, www.plantcell.org

Reconstitution of Plant Alkane Biosynthesis in Yeast Demonstrates That *Arabidopsis* ECERIFERUM1 and ECERIFERUM3 Are Core Components of a Very-Long-Chain Alkane Synthesis Complex[C][W]

Amélie Bernard,[a,b] Frédéric Domergue,[a,b] Stéphanie Pascal,[a,b] Reinhard Jetter,[c] Charlotte Renne,[d] Jean-Denis Faure,[d] Richard P. Haslam,[e] Johnathan A. Napier,[e] René Lessire,[a,b] and Jérôme Joubès[a,b,1]

[a] Université de Bordeaux, Laboratoire de Biogenèse Membranaire, Unité Mixte de Recherche 5200, F-33076 Bordeaux, France
[b] Centre National de la Recherche Scientifique, Laboratoire de Biogenèse Membranaire, Unité Mixte de Recherche 5200, F-33076 Bordeaux, France
[c] Departments of Botany and Chemistry, University of British Columbia, Vancouver, British Columbia V6T 1Z4, Canada
[d] Institut Jean-Pierre Bourgin, Unité Mixte de Recherche 1318, Institut National de la Recherche Agronomique AgroParisTech, Centre de Versailles-Grignon, F-78026 Versailles, France
[e] Rothamsted Research, Harpenden, Herts AL5 2JQ, United Kingdom

In land plants, very-long-chain (VLC) alkanes are major components of cuticular waxes that cover aerial organs, mainly acting as a waterproof barrier to prevent nonstomatal water loss. Although thoroughly investigated, plant alkane synthesis remains largely undiscovered. The *Arabidopsis thaliana* ECERIFERUM1 (CER1) protein has been recognized as an essential element of wax alkane synthesis; nevertheless, its function remains elusive. In this study, a screen for CER1 physical interaction partners was performed. The screen revealed that CER1 interacts with the wax-associated protein ECERIFERUM3 (CER3) and endoplasmic reticulum–localized cytochrome b5 isoforms (CYTB5s). The functional relevance of these interactions was assayed through an iterative approach using yeast as a heterologous expression system. In a yeast strain manipulated to produce VLC acyl-CoAs, a strict CER1 and CER3 coexpression resulted in VLC alkane synthesis. The additional presence of CYTB5s was found to enhance CER1/CER3 alkane production. Site-directed mutagenesis showed that CER1 His clusters are essential for alkane synthesis, whereas those of CER3 are not, suggesting that CYTB5s are specific CER1 cofactors. Collectively, our study reports the identification of plant alkane synthesis enzymatic components and supports a new model for alkane production in which CER1 interacts with both CER3 and CYTB5 to catalyze the redox-dependent synthesis of VLC alkanes from VLC acyl-CoAs.

INTRODUCTION

The aerial epidermis of terrestrial plants produces and secretes a mixture of very-long-chain (VLC) lipids that assemble into a waterproof barrier called the cuticle. Strategically located at the plant–air interface, the cuticle plays a critical role in the interactions between the plant and its environment. Besides its main function in preventing plant desiccation, the cuticle is also involved in plant protection from UV radiation, a self-cleaning process called the lotus effect, which limits the deposition of biotic and abiotic pollutants on plant surfaces, and protection against plant pathogens and insects (Shepherd and Wynne Griffiths, 2006). Furthermore, several lines of evidence have linked the cuticle to plant development processes, such as specialized epidermal cell differentiation and delimitation of organ boundaries (Javelle et al., 2011). The protective capacities of the cuticle are mainly based on physical and biochemical properties of its two highly hydrophobic components, cutin and cuticular waxes (Pollard et al., 2008; Domínguez et al., 2011). Overlying the epidermis cell wall, the first layer of the cuticle consists of cutin, a polyester of modified fatty acids and glycerol monomers, embedded with intracuticular waxes (Pollard et al., 2008; Li and Beisson, 2009); covering the cutin matrix, epicuticular waxes form the smooth or crystalloid outermost layer of the cuticle (Jeffree, 1996). Beyond the polymerized cutin, cuticular waxes mostly consist of a complex mixture of VLC aliphatic compounds, triterpenoids, as well as minor sterols and flavonoids (Buschhaus and Jetter, 2011). Aliphatic acyl chains of waxes derive from very-long-chain fatty acids (VLCFAs), with predominant chain lengths ranging from 26 to 32 carbons, resulting from the epidermal acyl-CoA elongase activity (Zheng et al., 2005; Bach et al., 2008; Joubès et al., 2008; Beaudoin et al., 2009). After elongation, acyl chains are processed according to two different biosynthetic routes: either the alcohol-forming pathway, yielding fatty alcohols and alkyl esters, or the alkane-forming pathway, generating fatty aldehydes, alkanes, and their derivatives (Samuels et al., 2008).

[1] Address correspondence to jjoubes@biomemb.u-bordeaux2.fr.
The author responsible for distribution of materials integral to the findings presented in this article in accordance with the policy described in the Instructions for Authors (www.plantcell.org) is: Jérôme Joubès (jjoubes@biomemb.u-bordeaux2.fr).
[C] Some figures in this article are displayed in color online but in black and white in the print edition.
[W] Online version contains Web-only data.
www.plantcell.org/cgi/doi/10.1105/tpc.112.099796

In the past 20 years, reverse genetic analyses of *Arabidopsis thaliana* mutants have provided significant advances in the understanding of wax metabolism (Kunst and Samuels, 2009). In fact, biosynthesis of compounds on the alcohol-forming pathway is now well described, because genes have been clearly identified, and the corresponding proteins have been functionally characterized (Rowland et al., 2006; Li et al., 2008). However, these approaches failed to uncover the enzymes involved in alkane synthesis, leaving the alkane-forming pathway poorly understood. Yet VLC alkanes dominate the wax mixture of many plant species, representing up to 70% of the total wax amount in *Arabidopsis* leaves, where they play critical roles in plant physiology, notably in pollen hydration and thus plant fertility, resistance to drought stress, and plant–pathogen interactions (Aarts et al., 1995; Kosma et al., 2009; Bourdenx et al., 2011). Moreover, because alkanes are the major constituents of liquid fuels, the discovery of the alkane biosynthetic machinery in plants would provide a toolbox of enzymes for the production of renewable hydrocarbon sources and the next generations of biofuels (Joyce and Stewart, 2011). Therefore, because of the importance of alkanes for both biotechnological purposes and plant physiological functions, the characterization of the plant VLC alkane–forming enzymes has been a challenging goal for decades (Jetter and Kunst, 2008; Kunst and Samuels, 2009).

Early biochemical analyses led to the proposal that alkanes could be produced from elongated acyl chains via intermediate aldehydes. This hypothesis was based on the observed conversion of C_{18} aldehyde into C_{17} alkane with the release of CO in pea (*Pisum sativum*) and a green algae (*Botryococcus braunii*), suggesting that a potential decarbonylation mechanism occurred (Cheesbrough and Kolattukudy, 1984; Dennis and Kolattukudy, 1991; Schneider-Belhaddad and Kolattukudy, 2000). Further characterization of the partially purified alkane synthesis activity in pea indicated that it requires metal ions and is inhibited by O_2 and reducing agents, suggesting that the reaction would be redox-independent (Schneider-Belhaddad and Kolattukudy, 2000). Because VLC aldehydes are found in the pool of cuticular waxes, it was proposed that VLCFAs could be reduced by a fatty acid reductase into corresponding even-numbered aldehydes, and then an aldehyde decarbonylase (AD) could catalyze the conversion into VLC alkanes with the loss of one carbon (Samuels et al., 2008). However, definitive evidence for intermediate aldehydes has never been provided, and enzymatic activities were never assessed. Interestingly, this putative biochemical mechanism can be compared with the long-chain alkane biosynthesis in the cyanobacteria *Synechococcus* sp and *Nostoc punctiforme*. Indeed, the microbial mechanism was recently reported to proceed via a two-step pathway from acyl–Acyl Carrier Protein (ACP) precursors to an aldehyde intermediate and the hydrocarbon product involving two enzymes, an acyl reductase and an aldehyde decarbonylase (Schirmer et al., 2010; Das et al., 2011).

The analysis of the *Arabidopsis eceriferum1* (*cer1*) mutant indicated the involvement of the corresponding protein in alkane biosynthesis. Indeed, the *cer1* mutant is characterized by a nearly depleted load of alkanes and their derivates accompanied by a slight increase in aldehyde content (Koornneef et al., 1989; Aarts et al., 1995; Jenks et al., 1995; Bourdenx et al., 2011). Support for the central role of CER1 in alkane production was provided by the recent characterization of *Arabidopsis* transgenic lines, in which *CER1* overexpression led to a large and specific accumulation of wax VLC alkanes (Bourdenx et al., 2011). Consistent with such an involvement in wax metabolism, *CER1* expression was found confined to the epidermis of aerial organs and the CER1 protein located to the endoplasmic reticulum (ER), where wax biosynthesis takes place (Kamigaki et al., 2009; Bourdenx et al., 2011). CER1 is a membrane-bound protein that shares no significant sequence similarity with functionally characterized proteins, except for a short sequence containing a tripartite His-rich motif $HX_3H+HX_2HH+HX_2HH$ (Aarts et al., 1995). His-rich clusters are part of the di-iron catalytic core found in a large family of integral membrane enzymes involved in fatty acid metabolism (Shanklin and Cahoon, 1998). Therefore, it has been suggested that CER1 could have an enzymatic activity associated with alkane production (i.e., that CER1 could be the alkane-forming enzyme [Aarts et al., 1995]). This hypothesis is further supported by the characterization of the ADs from cyanobacteria, which belong to a family of soluble nonheme di-iron carboxylate enzymes (Schirmer et al., 2010). Nevertheless, the function of CER1 has never been provided, partly because of the lack of information about VLC alkane–forming activity at the molecular level, the unknown substrate, and the low solubility and unavailability of commercial VLC aldehydes. Furthermore, because expression of CER1 in heterologous systems did not lead to production of alkanes (Bourdenx et al., 2011), the CER1 function remains a crucial open question for the understanding of VLC alkane formation.

In this article, the CER1 protein was used as a starting point to reconstitute the plant alkane–forming pathway. To learn more about CER1 function, an exploratory screen was conducted to identify CER1 physical interaction partners. In both yeast and plant cells, CER1 was found to interact with the wax-associated protein CER3 and with the cytochrome b5 isoforms (CYTB5s) serving as ER-reducing components. Through an iterative approach performed in a yeast heterologous system producing VLC acyl-CoAs, we showed that a mandatory CER1/CER3 coexpression results in VLC alkane production, thus identifying the enzymatic components catalyzing plant alkane synthesis. *Arabidopsis* CYTB5s were found to increase alkane production, and analysis of point-mutated CER1 and CER3 proteins suggested that CYTB5s are specific CER1 cofactors, highlighting a potential redox-dependent CER1 activity for alkane synthesis. Taken together, our results elucidate the plant alkane–forming pathway and support a new model for alkane synthesis in which CER1 and CER3 constitute the core components of a multiprotein enzymatic complex catalyzing the redox-dependent conversion of VLC acyl-CoAs to VLC alkanes.

RESULTS

CER1 Physically Interacts with Itself, CER3, and the ER-Associated CYTB5 Isoforms

Because all previous attempts to characterize CER1 activity by heterologous expression had failed (Bourdenx et al., 2011), we

hypothesized that protein partners might be needed for CER1 to function. To find such partners, CER1 potential interactions with proteins that are involved in wax synthesis but with an unknown function were first assessed. Even though several *Arabidopsis cer* mutants with decreased wax alkane amounts similar to *cer1* mutants have been reported, only the *CER2*, *CER3/WAX2*, *CER5/ABCG12*, *CER6/KCS6*, *CER7*, *CER8/LACS1*, and *CER10/ECR* genes have been cloned (Samuels et al., 2008). Most of the corresponding proteins are involved in wax formation, but not directly in alkane biosynthesis, leaving CER3 as the only currently available candidate with a putative function in alkane formation (Chen et al., 2003). The potential physical interaction of CER1 with CER3 was tested using a split-ubiquitin yeast two-hybrid (SUY2H) assay with Cub-CER1 as bait and NubG-CER3 as prey (Figure 1). Unlike yeast cells coexpressing Cub-CER1 and NubG as a negative control, the yeast coexpressing Cub-CER1 and NubG-CER3 were able to grow on the different selective media and show β-galactosidase activity, indicating that CER3 interacts with CER1 (Figure 1). Analysis of the yeast coexpressing Cub-CER1 as bait and NubG-CER1 as prey showed that, in yeast, CER1 also interacts with itself, suggesting that CER1 could dimerize in plant cells.

To identify other CER1 partners, an exploratory screen was then conducted in the SUY2H system. Because *CER1* expression is confined to the epidermis cells, where the entirety of wax metabolism takes place, a cDNA library was constructed in the SUY2H prey expression vector using RNA of epidermis peeled from *Arabidopsis* stems. The screen of the generated epidermis cDNA library with Cub-CER1 as bait isolated 320 clones, which were further selected for their ability to grow on the different stringent media as well as for their β-galactosidase activity. Furthermore, because CER1 locates to the ER, all candidate proteins that have been experimentally and unequivocally associated with subcellular compartments other than the ER and the cytosol were considered false positive (representing 20% of the clones). All together, this analysis led to the selection of 96 positive clones, in which 30% of the isolated proteins were found to be related to lipid metabolism. Interestingly, the screen notably isolated three CYTB5 proteins (CYTB5-B [*At2g32720*], CYTB5-C [*At2g46650*], and CYTB5-D [*At5g48810*]) as potential CER1 partners (representing up to 15% of the isolated clones). CYTB5s are ubiquitous hemoproteins that act as electron transfer components to nonheme irons associated with His clusters of ER-localized enzymes (Shanklin and Cahoon, 1998). Although early biochemical analyses proposed that the plant alkane–forming activity is redox-independent (Cheesbrough and Kolattukudy, 1984; Schneider-Belhaddad and Kolattukudy, 2000), the presence of His-clusters in the CER1 amino acid sequence suggests that CYTB5 proteins could be CER1 cofactors. Therefore, these candidate proteins were selected for further analyses. A targeted SUY2H assay confirmed the interaction of CYTB5-B, CYTB5-C, and CYTB5-D with CER1 and also indicated the interaction of CER1 with the fourth potentially ER-associated CYTB5-E isoform (Figure 1).

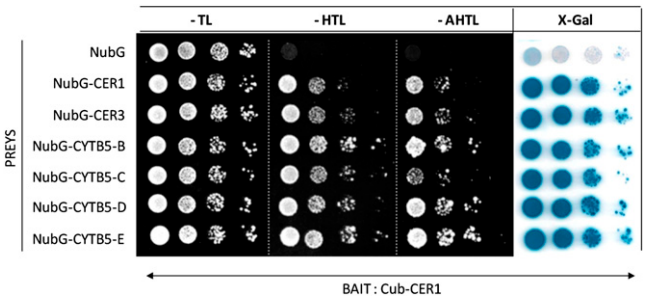

Figure 1. CER1 Interacts with Itself, CER3, and CYTB5s in the SUY2H System.

Yeast cells cotransformed with Cub-CER1 as bait and NubG-CER1, NubG-CER3, or NubG-CYTB5 isoforms as prey are able to grow on stringent media lacking His, Leu, Trp (−HTL), and adenine (−AHTL), and show β-galactosidase activity (X-Gal), whereas cells cotransformed with Cub-CER1 and empty prey vector (NubG) as negative control do not (OD_{600} yeast cells: 10^{-1}; 10^{-2}; 10^{-3}; 10^{-4}).
[See online article for color version of this figure.]

To test CER1 interaction with candidate proteins in plant cells, we performed an *Arabidopsis* transient split-luciferase assay (Van Leene et al., 2010). In this system, the firefly luciferase (LUC) protein is split into two halves, which are fused to the bait and prey proteins. In plant cells, coexpression of the fusion proteins will reconstitute LUC activity if, and only when, the proteins of interest interact. Cotyledons of *Arabidopsis* seedlings were cotransformed with constructs for expression of CER1 fused to the N-terminal part of the firefly LUC protein (NterLUC-CER1), and candidate partners fused to its C-terminal part (CterLUC-PREY). Two ER-localized proteins that are not implicated in wax production, At-DPL1 (LCB-1P lyase) and At-SUR2B (LCB hydroxylase), were used as negative control prey. Significant luciferase activity was observed only in seedlings expressing NterLUC-CER1 together with CterLUC-CER1, CterLUC-CER3, CterLUC-CYTB5-B, CterLUC-CYTB5-C, CterLUC-CYTB5-D, or CterLUC-CYTB5-E, indicating that CER1 interacts with all these proteins in *Arabidopsis* cells (Figure 2A).

Previous studies had shown that both CER1 and CER3 proteins are located to the ER (Kamigaki et al., 2009). Similarly, *Arabidopsis* CYTB5-B and CYTB5-D are known to be located to the ER (Maggio et al., 2007; Nagano et al., 2009), and based on sequence similarity, CYTB5-C and CYTB5-E were predicted also to be located there (Hwang et al., 2004). To verify this prediction, green fluorescent protein (GFP)-CER1 and yellow fluorescent protein (YFP)-CYTB5 fusion proteins were transiently coexpressed in *Arabidopsis* seedlings. Confocal microscopy analysis showed that CYTB5-B and CYTB5-D, as well as CYTB5-C and CYTB5-E, colocalized with CER1, illustrating how these proteins interact with CER1 in plant cells (Figure 2B).

Reconstitution of the VLC Alkane–Forming Pathway in Yeast

The finding that CER1 physically interacts with CER3 and CYTB5(s) suggested that these proteins could participate with CER1 in alkane production. To test this hypothesis, an iterative approach was conducted in yeast, an organism that does not naturally produce alkanes. Lipid analyses of engineered yeasts expressing CER1, CER3, and CYTB5-B genes in all single, double, and triple combinations never showed any difference when compared with the control yeast transformed with

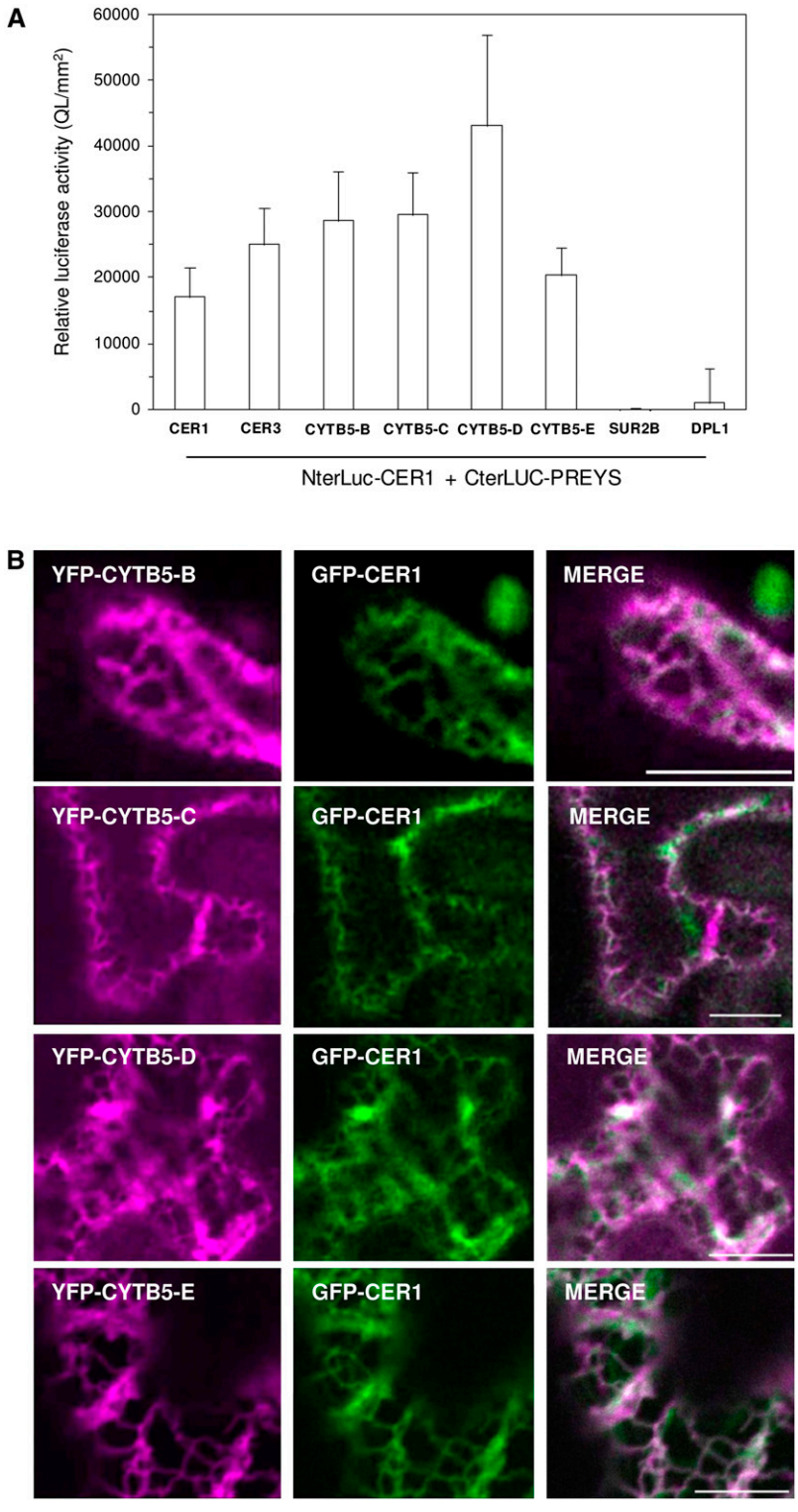

Figure 2. CER1 Physically Interacts with Itself, CER3, and CYTB5s in *Arabidopsis* Cells.

(A) Relative light emission measurements of the different NterLUC-CER1/CterLUC-PREY pairs coexpressed in *Arabidopsis* seedlings indicate an interaction between CER1 and itself, CER3, and CYTB5s in *Arabidopsis* cells. At-DPL1 (LCB-1P lyase) and At-SUR2B (LCB hydroxylase) were used as negative control prey. Relative luciferase activity is expressed in quanta of light (QL)/mm^2. The data represent mean values with corresponding SD values ($n \geq 4$; $n = 2$ for negative controls).

(B) Confocal images of *Arabidopsis thaliana* cotyledons transiently cotransformed with GFP-CER1 and YFP-CYTB5s as indicated in the legend. YFP-CYTB5s are localized to the ER (left panel) where they colocalized with GFP-CER1 (central panel) in the merge (right panel).

Bars in **(B)** = 10 μm.

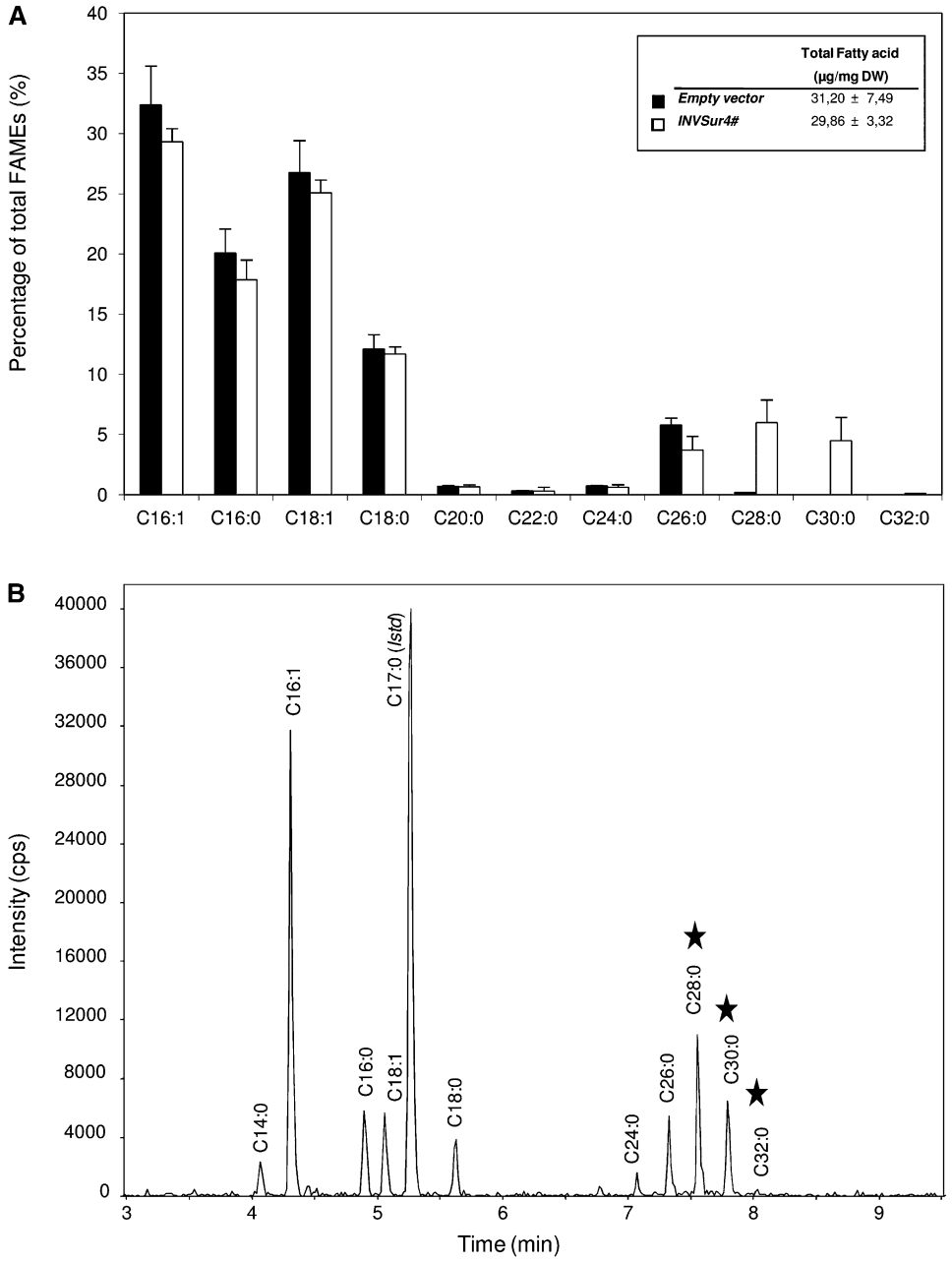

Figure 3. The Wild-Type Yeast Strain (INVSc1) Transformed with the Mutated SUR4 F262K/K266L (SUR4#) Protein Shows Production of VLC Fatty Acids and VLC Acyl-CoAs.

(A) Comparison of the FAME profile of INVSc1 control strain (transformed with empty vector) with INVSur4# (INVSc1 transformed with Sur4#) shows that expression of SUR4# in wild-type yeast triggers an overaccumulation of C28 fatty acids as well as the synthesis of C30 and C32 fatty acids. Mean values (%) of percentage of total FAMEs are given with SD ($3 \leq n \leq 14$). Each FAME species is designated by carbon chain length and degrees of unsaturation. The C17:0 fatty acid was used as internal standard. Insert: mean values are expressed in µg per mg of dry weight (DW) of total fatty acids as FAMEs with SD ($3 \leq n \leq 14$).

(B) The chromatogram of the INVSur4# strain acyl-CoA pool indicates the production of VLC acyl-CoAs (highlighted by stars). Each acyl-CoA is designated by carbon chain length and degrees of unsaturation. C17:0 acyl-CoA was used as internal standard. Intensity is expressed in counts per second (cps).

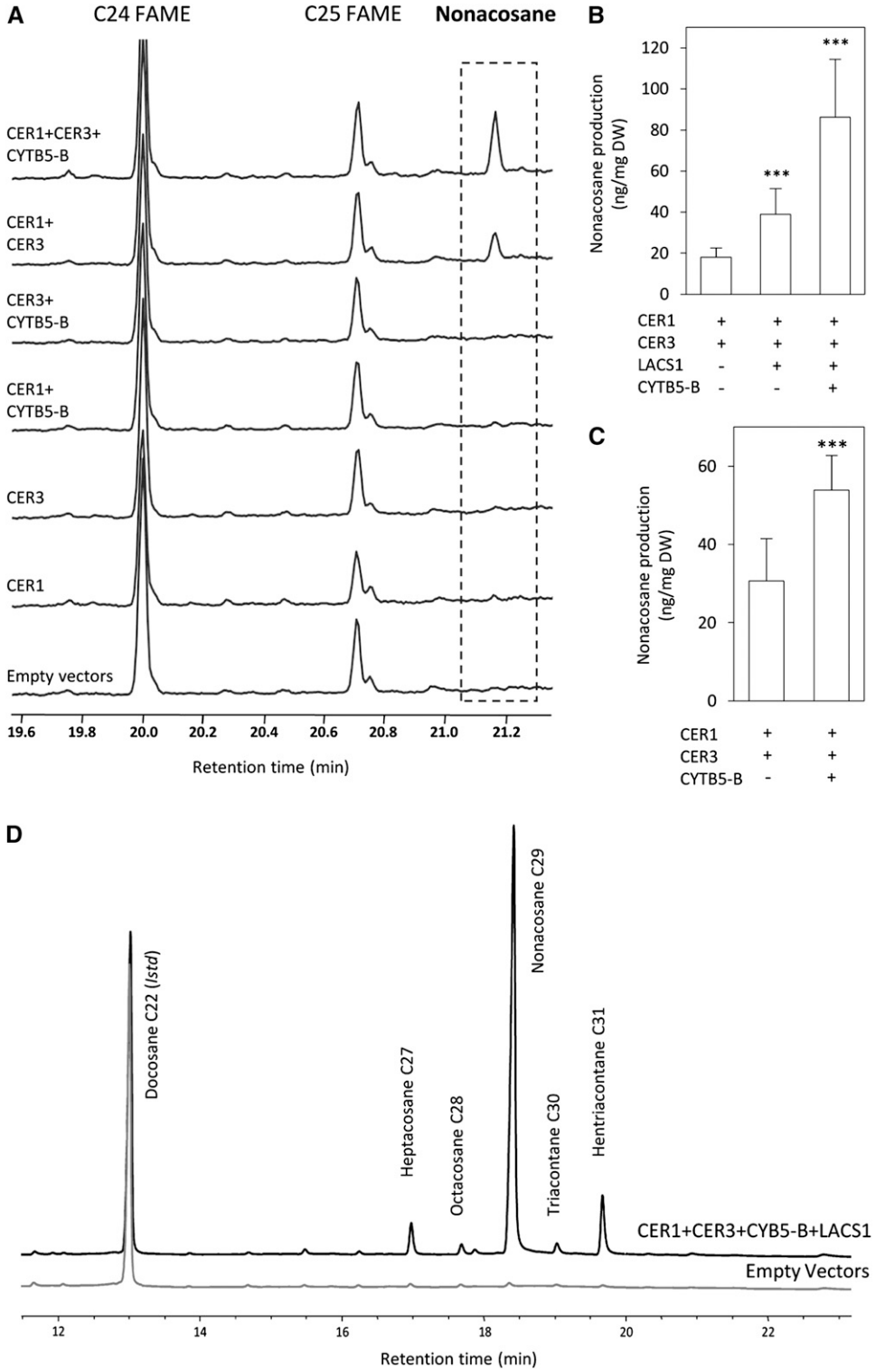

Figure 4. Synthesis of VLC Alkanes in INVSur4# Yeast Coexpressing Various Combinations of CER1 Together with CER3, CYTB5-B, and LACS1.

(A) The INVSur4# yeast coexpressing *Arabidopsis* CER1 and CER3 has the ability to synthesize nonacosane. Additional coexpression of CYTB5-B enhances nonacosane production. GC-MS traces of total fatty acyl chain analyses of INVSur4# cotransformed with denoted *Arabidopsis* transgenes or with corresponding empty vectors as control.

corresponding empty vectors. Our previous work had shown that overexpression of *CER1* in *Arabidopsis* leads to a specific increase of alkanes with carbon chain lengths between 27 and 33 carbon atoms, suggesting that CER1 likely has chain length specificity for substrates with 28 to 34 carbon atoms (Bourdenx et al., 2011). However, wild-type yeast produces VLCFAs only up to C26 (with traces of C28) (Figure 3A). Therefore, the wild-type yeast strain was manipulated to generate a system where significant amounts of CER1 potential substrates were accessible. For that purpose, we used the mutated yeast elongase component SUR4 F262K/K266L (SUR4#), which had been shown to allow production of C28 and C30 fatty acids in *sur4*Δ mutant yeast (Denic and Weissman, 2007). Gas chromatography–mass spectrometry (GC-MS) and liquid chromatography–tandem mass spectrometry analyses of fatty acid methyl esters (FAMEs) and acyl-CoAs, respectively, confirmed that SUR4# expression in wild-type yeast (engineered yeast hereafter referred to as INVSur4#) resulted in the production of substantial amounts of C28 and C30 as well as traces of C32 acyl compounds (Figures 3A and 3B).

When CER1 or CER3 alone was expressed in INVSur4#, alkanes could not be detected (Figure 4A). By contrast, when CER1 was expressed together with CER3 in INVSur4#, a new lipid was detected and identified as nonacosane (C29 alkane) by GC-MS (Figure 4A). No other modification of the fatty acid profile was observed (see Supplemental Figures 1A and 1D online), and no alkane was found in the yeast medium. Taken together, these results indicate that CER1 and CER3 are both necessary and sufficient for VLC alkane synthesis in VLCFA-producing yeast.

The engineered yeast system developed was then used to investigate the substrates used by CER1/CER3 to produce alkanes. Indeed, although it is well established that VLC alkanes derive from elongated acyl chains (Samuels et al., 2008), it is still unclear whether VLCFAs or acyl-CoAs are the true alkane precursors. To address this question, we used the *Arabidopsis* Long-Chain Acyl-CoA Synthetase1 (LACS1), which performs the conversion of fatty acids into their activated CoA thioesters with high in vitro specificity for C30 fatty acids (Lü et al., 2009). The coexpression of LACS1 together with CER1 and CER3 in INVSUR4# led to a 2-fold increase in nonacosane amount over the lines coexpressing only CER1 and CER3 (Figure 4B; see Supplemental Figures 1B to 1D online), supporting that VLC acyl-CoAs are precursors for VLC alkane synthesis.

To test the relevance of CER1 interaction with CYTB5s for alkane synthesis, CYTB5-B was then coexpressed with CER1 and CER3 in INVSur4#. When compared with the yeast INVSur4# coexpressing only CER1 and CER3, the additional presence of CYTB5-B led to an almost 2-fold increase in nonacosane production (Figures 4A to 4C; see Supplemental Figures 1A and 1D online), suggesting that CYTB5s are cofactors of a redox-dependent CER1/CER3 activity for VLC alkane synthesis in *Arabidopsis*.

CER1/CER3 alkane-forming activity was further characterized by scaling up yeast cultures and separating the hydrocarbon fraction from the total lipid extract on thin layer chromatography (TLC). Gas chromatography–flame ionization detection (GC-FID) and GC-MS analyses showed that the resulting fraction contained mainly nonacosane (C29) together with heptacosane (C27) and hentriacontane (C31) as well as traces of octacosane (C28) and triacontane (C30) (Figure 4D; see Supplemental Figure 2 online). Thus, the alkanes synthesized by CER1/CER3 in yeast match the chain length specificity observed in planta, as shown in *Arabidopsis CER1*-overexpressing lines (Bourdenx et al., 2011). Collectively, these results demonstrate that CER1 and CER3 constitute the enzymatic core components of plant alkane biosynthesis. Moreover, yeast cells coexpressing CER1/CER3 together with CYTB5-B and LACS1 produce an average of 86 ng of nonacosane per mg of dry weight. This yield corresponds to ~1 and 64% of the amount produced by *Arabidopsis* stem (6900 ± 324 ng per mg of dry weight) or rosette leaves (135 ± 28 ng per mg of dry weight), respectively.

The CER1 His-Rich Motifs Are Essential for VLC Alkane Synthesis

His clusters have been shown to be essential for the catalytic activity of hydroxylase and desaturase enzymes, where they serve as ligands for a di-iron binding site mediating electron transfer from CYTB5s (Shanklin and Cahoon, 1998). Therefore, the functional relevance of the CER1 His clusters was assayed by generating mutated CER1 proteins in which a conserved His in each of the three motifs was replaced by an Ala (Figure 5A). When the CER1 mutants were coexpressed in INVSur4# together with CER3 and CYTB5-B, no alkanes were detected (Figure 5B; see Supplemental Figure 3 online), indicating that all three CER1 His-rich clusters are essential for alkane synthesis. To verify this result in planta, two CER1 His mutants were overexpressed in the *Arabidopsis cer1-1* knockout mutant

Figure 4. (continued).

(B) and **(C)** Quantitative analysis of nonacosane production shows that *Arabidopsis* LACS1 **(B)** and CYTB5-B **([B]** and **[C])** enhance alkane production when coexpressed together with CER1 and CER3 in INVSur4#.

(B) Yeast cells were grown in stringent medium lacking His, Trp, Leu, and uracil. Mean values of nonacosane (ng/mg of dry weight [DW]) are given with SD ($6 \leq n \leq 8$). Significance was assessed by Student's *t* test (***, $P < 0.01$).

(C) Yeast cells were grown in stringent medium lacking Trp, Leu, and uracil. Mean values of nonacosane are expressed in ng per mg of dry weight with SD ($n = 14$). Significance was assessed by Student's *t* test (***, $P < 0.01$).

(D) The INVSur4# yeast coexpressing *Arabidopsis* CER1, CER3, CYTB5-B, and LACS1 produces VLC alkanes with chain lengths ranging from 27 to 31 carbon atoms. INVSur4# control strain (transformed with empty vectors) shows no alkane production. GC-FID traces of the hydrocarbon fractions after separation from total lipid extract by TLC. Docosane (20 μg) was used as internal standard.

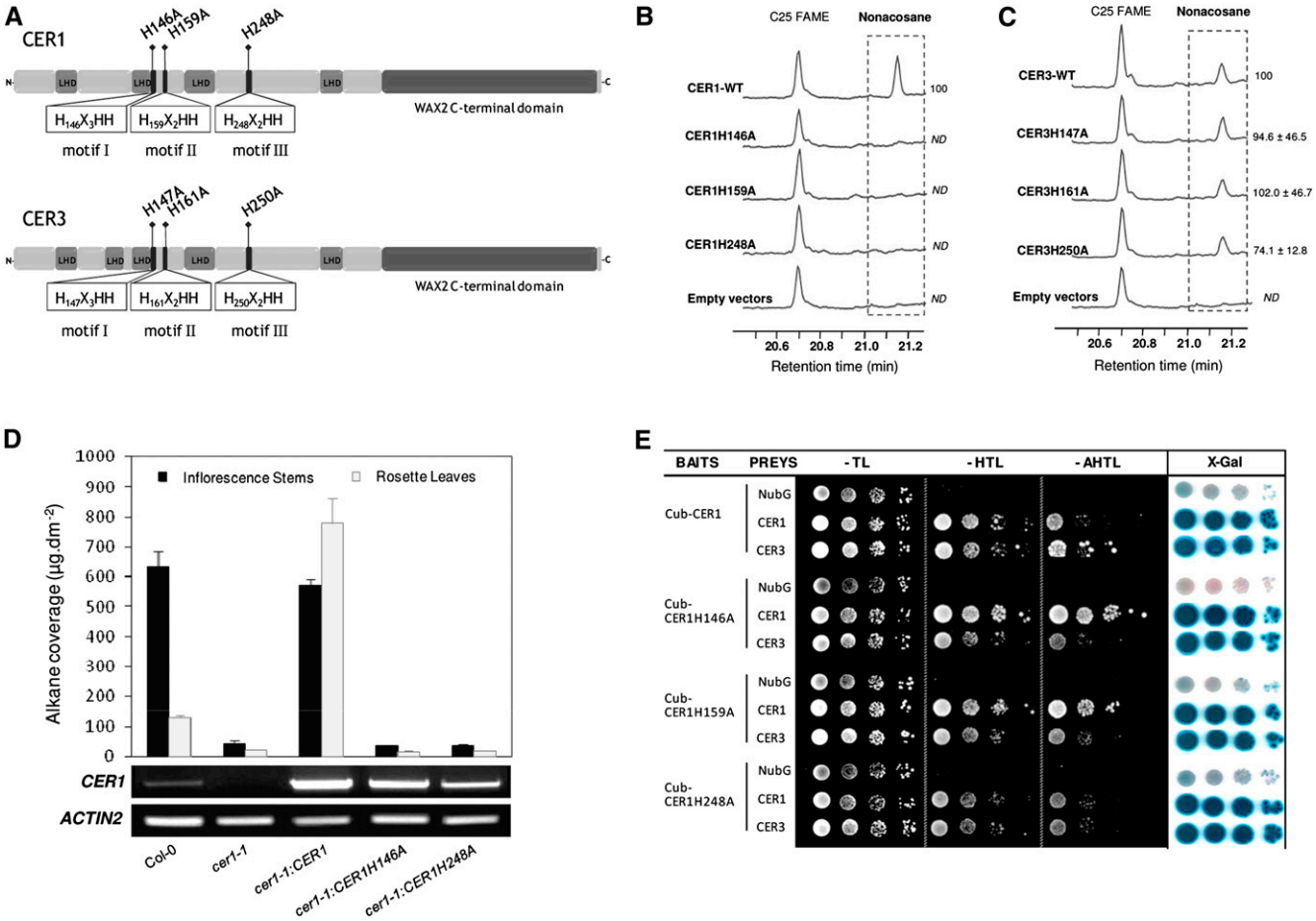

Figure 5. Functional Relevance of His-Rich Motifs in *Arabidopsis* CER1 and CER3.

(A) Schematic representation of CER1 and CER3 primary protein structures indicating the positions of the three His-rich motifs and the WAX2 C-terminal domain. Residue number of the His replaced by an Ala is indicated. LHD, long hydrophobic domain.

(B) Coexpression of CER1 His mutants together with CER3 and CYTB5-B in INVSur4# does not lead to nonacosane production, in contrast with coexpression of wild-type (WT) CER1 with CER3 and CYTB5-B.

(C) Coexpression of CER3 His mutants together with CER1 in INVSur4# does not lead to modification in nonacosane production compared with coexpression of wild-type CER3 with CER1. GC-MS traces of total fatty acyl chain analyses of INVSur4# cotransformed with *Arabidopsis* transgenes as detailed in the legend or with corresponding empty vectors as control. Mean values of nonacosane quantities (%) relative to the wild-type CER1 or CER3 averages are given with SD ($n = 5$). ND, not detected.

(D) Molecular and phenotypic characterization of His-mutated CER1-overexpressing *Arabidopsis* lines. Alkane amounts of wild-type Col-0, *cer1-1*, *cer1-1*:*CER1*, *cer1-1*:*CER1H146A*, and *cer1-1*:*CER1H248A Arabidopsis* lines are expressed as µg dm^{-2} stem or leaf surface area (Top). The data represent means ± SD ($n = 3$). RT-PCR analysis of steady state *CER1* transcripts in leaves of 6-week-old plants of the different lines compared with the wild-type plants as indicated (Bottom). The *ACTIN2* gene was used as a constitutively expressed control.

(E) CER1 His mutants interact with CER1 and CER3 in the SUY2H system. Yeast cells cotransformed with Cub-CER1, Cub-CER1H146A, Cub-CER1H161A, or Cub-CER1H248A as bait and NubG-CER1 or NubG-CER3 as prey are able to grow on stringent media lacking His, Leu, Trp (−HTL), and adenine (−AHTL) and show β-galactosidase activity, whereas cells cotransformed with each bait and empty prey vector (NubG) as negative control do not (OD yeast cells: 10^{-1}; 10^{-2}; 10^{-3}; 10^{-4}).

[See online article for color version of this figure.]

(*cer1-1*:*CER1H146A*; *cer1-1*:*CER1H248A*) and compared with a transgenic line overexpressing the wild-type *CER1* gene (*cer1-1*:*CER1*). Although no *CER1* transcripts were detected in the *cer1-1* mutant, both His mutant lines and the *cer1-1*:*CER1* line exhibited higher levels of transcripts than wild-type plants (Figure 5D). Gas chromatography analyses showed that overexpression of the wild-type *CER1* in the *cer1-1* background restored alkane biosynthesis, whereas overexpression of *CER1H146A* or *CER1H248A* was not able to rescue the wild-type phenotype (Figure 5D; see Supplemental Figures 4 and 5 and Supplemental Tables 1 and 2 online). Taken together, these results demonstrate that the His-rich motifs are essential for CER1 to function. Furthermore, SUY2H assays performed with CER1 mutated proteins as baits showed that the mutations in

CER1 His clusters do not prevent CER1/CER1 or CER1/CER3 interactions (Figure 5E). These data indicate that the absence of alkane synthesis observed with the CER1 mutants is caused by a defect in CER1 activity rather than the incorrect formation of the CER1/CER3 complex, thereby demonstrating that CER1 His-rich motifs are part of the catalytic site of the enzyme.

Interestingly, CER3 also contains a tripartite His cluster built around eight conserved histidines (Figure 5A) (Chen et al., 2003; Rowland et al., 2007). We further generated three CER3 mutants in which one conserved His in each of the three motifs (equivalent in position to those mutated in CER1) was replaced by an Ala (Figure 5A). Coexpression of CER3 mutated proteins together with CER1 in INVSur4# resulted in no obvious modification of nonacosane production as compared with CER3 wild-type coexpression (Figure 5C; see Supplemental Figure 6 online). Collectively, our findings suggest that the His clusters are part of the CER1 catalytic site but are not strictly required for CER3 activity.

DISCUSSION

CER1 and CER3 Functionally Interact to Produce VLC Alkanes

Even though strong evidence for *Arabidopsis* CER1 involvement in alkane biosynthesis had been provided (Aarts et al., 1995; Bourdenx et al., 2011), the function of this protein has never been elucidated. Because expression of CER1 alone is not sufficient to produce alkanes in heterologous systems, we speculated that CER1 might need protein partners for its activity. In this study, we report that CER1 physically interacts with CER3 in both yeast and *Arabidopsis*, suggesting that they associate to form an enzymatic complex. A strict expression of the CER1/CER3 complex in VLCFA-producing yeast leads to the synthesis of VLC alkanes, demonstrating that both proteins are required for the catalytic production of alkanes. Taken together, these results demonstrate that CER1 and CER3 are core components of the VLC alkane–forming enzymatic activity.

Toward the Understanding of the VLC Alkane–Forming Catalytic Activities

Based on early biochemical data (Cheesbrough and Kolattukudy, 1984; Schneider-Belhaddad and Kolattukudy, 2000) and on the analyses of *Arabidopsis cer1* and *cer3/wax2* mutant phenotypes (Aarts et al., 1995; Chen et al., 2003), a two-step pathway for VLC alkane synthesis was proposed, in which CER3 catalyzes the reduction of VLC acyl-CoAs generating intermediate fatty aldehydes that are subsequently decarbonylated by CER1 to VLC alkanes. Although it has been proposed that fatty aldehydes are intermediates of alkane formation in eukaryotes, such as insects and plants (Reed et al., 1994; Schneider-Belhaddad and Kolattukudy, 2000), the corresponding two-step pathway for long-chain alkane biosynthesis has been demonstrated only in cyanobacteria (Schirmer et al., 2010). In the microbial pathway, a fatty acyl-ACP reductase (FAAR) catalyzes the reduction of fatty acyl-ACPs to intermediate aldehydes, which are then used by an AD to produce alkanes (Schirmer et al., 2010; Das et al., 2011). Nevertheless, whereas the FAAR and AD from cyanobacteria do not share any common motifs with each other; *Arabidopsis* CER1 and CER3 are highly related. Sequence similarity and conserved intron positions in *CER1* and *CER3* indicate a common origin from the same ancestor gene (Sturaro et al., 2005). Furthermore, the two proteins share 35% identity (see Supplemental Figure 7 online), including elements analogous to both cyanobacterial proteins. Indeed, CER1 and CER3 both possess a conserved tripartite His motif serving as ligand for a di-iron active site cluster in the catalytic site of several fatty acid–related membrane-bound enzymes (Shanklin et al., 1997; Shanklin and Cahoon, 1998; Idkowiak-Baldys et al., 2003). His clusters constitute the conserved feature of integral membrane oxygenases and oxidases and are equivalent to the carboxylate bridge di-iron cluster of their functionally related soluble homologs. Therefore, even though the plant and microbial proteins do not share sequence similarity, both CER1 and CER3 resemble the cyanobacterial AD, which was found to be structurally and

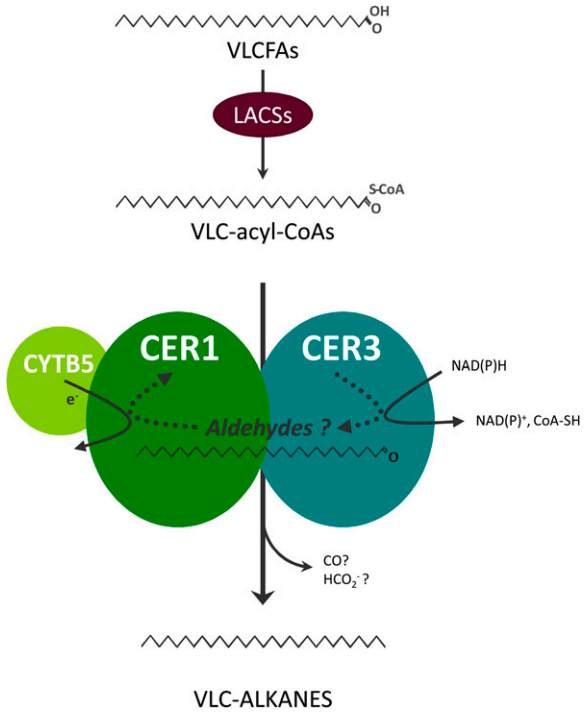

Figure 6. Proposed Biochemical Model in Which *Arabidopsis* CER1 and CER3 Act Synergistically for VLC Alkane Synthesis.

The results obtained in this study lead us to propose that the CER1 and CER3 proteins would form an enzymatic complex catalyzing the conversion of VLC acyl-CoAs to VLC alkanes. VLCFAs activated by the long-chain acyl CoA synthases (LACSs) in VLC acyl-CoAs would be used as precursors of VLC alkane synthesis. A mandatory CER1/CER3 heterodimer would efficiently catalyze a two-step reaction starting with the reduction of acyl-CoA to a potential intermediate aldehyde subsequently decarbonylated to alkane with the loss of one carbon potentially in carbon monoxide or formate as reported in cyanobacteria (Li et al., 2008). CYTB5s would interact with the di-iron catalytic core of CER1, providing electron(s) required for the decarbonylation reaction.
[See online article for color version of this figure.]

functionally related to nonheme di-iron enzymes (Das et al., 2011; Li et al., 2011). In addition, CER1 and CER3 possess the functionally uncharacterized WAX2 domain at their C termini (Figure 5A; see Supplemental Figure 7 online) that we also partially identified at the C terminus of the cyanobacterial FAAR protein (see Supplemental Figure 7 online). Interestingly, a mutation in the WAX2 domain of the CER3 protein was reported to severely inhibit wax synthesis in the *Arabidopsis cer3-4* mutant, suggesting that this domain is required for plant alkane biosynthesis (Rowland et al., 2007). In our study, we showed that the CER3 His clusters are nonessential for alkane synthesis but are crucial for CER1 function in both *Arabidopsis* and yeast. This supports the hypothesis that CER1 acts as an AD. Conversely, CER3 would be essential for alkane production by providing fatty aldehydes or another yet to be described metabolic intermediate to CER1. Alternatively, it is plausible that the two proteins possess a weak capacity for both reactions, with CER3 acting preferentially as the fatty acyl reductase and CER1 as the AD. The finding that CER1 and CER3 interact in both yeast and *Arabidopsis* suggests that the two proteins could act synergistically (i.e., that heterodimerization of CER1 and CER3 is necessary for efficient activity of both proteins). Thus, in the absence of its partner, either CER1 or CER3 could homodimerize to perform weak conversion of acyl-CoAs to alkanes. This could explain the phenotypes of the *cer3/wax2* and *cer1* null mutants, which are not completely devoid of aldehydes and alkanes (Chen et al., 2003; Bourdenx et al., 2011) as well as the synergistic effect of both mutations on trichome development observed in the *cer1 cer3* double mutant (Kurata et al., 2003). Technical limitations notwithstanding, further support for CER1/CER3 synergy is provided by the fact that no change in the fatty acyl composition was detected when only CER3 was expressed in yeast. In this context, significant amounts of aldehyde would be produced only when CER1 and CER3 are coexpressed in yeast but not detected, because they are converted into alkanes rather than accumulating. Thus, from our results, we propose a model in which a mandatory CER1/CER3 heterodimer would highly efficiently perform conversion of VLC acyl-CoAs to VLC alkanes (Figure 6).

CYTB5s as Electron Transfer Components for VLC Alkane Synthesis

In an attempt to identify new proteins involved in VLC alkane synthesis, we found that CER1 interacts with the entire subfamily of ER-associated *Arabidopsis* CYTB5s. CYTB5s act as electron transfer components to nonheme irons associated with His clusters of several ER-localized enzymes (Shanklin and Cahoon, 1998). Interestingly, coexpression of CYTB5-B together with CER1 and CER3 in yeast increased nonacosane production, suggesting an involvement of these proteins in VLC alkane formation in *Arabidopsis*. Because coexpression of CER1 and CER3 is sufficient for alkane synthesis in the engineered VLC acyl-CoA–synthesizing yeast, we hypothesize that reducing components must be provided by endogenous yeast CYTB5s. Mutagenesis analysis indicated that His-rich motifs are essential for CER1 activity but not for CER3, indicating that CYTB5s are likely to be cofactors specific for CER1 activity for VLC alkane formation. These results do not support the function of CER1 as a potentially redox-neutral decarbonylase proposed by early biochemical studies (Cheesbrough and Kolattukudy, 1984; Vioque and Kolattukudy, 1997; Schneider-Belhaddad and Kolattukudy, 2000). However, recent work on cyanobacterial alkane biosynthesis showed that, in vitro, long-chain aldehyde decarbonylation, catalyzed by a di-iron enzyme, strictly requires a reducing system to produce alkanes in both O_2-dependent and -independent reactions (Das et al., 2011; Li et al., 2011). Based on these latest mechanisms and our data, we propose that CYTB5 act as a cofactor of redox-dependent CER1 activity in the CER1/CER3 VLC alkane–forming complex. It is interesting to note that reducing equivalents are apparently delivered to the cyanobacterial AD by the ferredoxin/ferredoxin reductase system (Schirmer et al., 2010) which is shared by several soluble nonheme di-iron enzymes, whereas, for the plant alkane–forming activity, this role could be played by the CYTB5s—and presumably the CYTB5 reductase—used by the ER membrane-bound nonheme di-iron enzymes (Sperling et al., 2003).

The early characterization of *Arabidopsis cer1* and *cer3* mutant phenotypes (Koornneef et al., 1989) pointed to the involvement of the corresponding proteins as components of wax metabolism. Nevertheless, the cloning of CER1 and CER3 was not sufficient to reveal their biochemical activity, leaving the VLC alkane synthesis unresolved. This study reports VLC alkane production in a heterologous yeast system, demonstrating the catalytic functions of CER1 and CER3 for VLC alkane production and thus identifying the enzymatic components of plant alkane synthesis. Further manipulations of the engineered yeast suggest a model for plant VLC alkane metabolism in which VLC acyl-CoAs would serve as precursors of a CYTB5s/CER1/CER3 complex for redox-dependent VLC alkane synthesis. The reconstitution of *Arabidopsis* VLC alkane biosynthesis in yeast provides an excellent tool for further understanding wax metabolism. Furthermore, production of VLC alkanes in yeast lays the foundation for conceptual and metabolic manipulation of this and other organisms toward large-scale production of tomorrow's biofuels.

METHODS

Plant Material and Conditions

Arabidopsis thaliana plants (ecotype Columbia [Col-0]) were cultivated under optimal growth conditions as previously described (Joubès et al., 2008). The *cer1-1* T-DNA insertion line (SALK_008544) and the *cer1-1*:*CER1* transgenic line have been previously described (Bourdenx et al., 2011). *Landsberg erecta Arabidopsis* seedlings were used for transient split-luciferase assays as described in Van Leene et al. (2010).

Cloning and Transgenic Yeasts

Site-directed mutagenesis was performed as previously described (Taton et al., 2000) with minor modifications. His codons were replaced by the Ala codon GCT. Primers used for generation of mutation-containing fragments are detailed in Supplemental Tables 3 and 4 online. *CER1*, His-mutated *CER1s*, *CER3*, His-mutated *CER3s*, *LACS1*, and *CYTB5-B* open reading frames were amplified by PCR using primers detailed in Supplemental Table 4 online and cloned into yeast expression vectors as

detailed in Supplemental Table 4 online. SUR4-F262A/K266L cloned in p416 MET25-FLAG3 was used as previously described (Denic and Weissman, 2007). *Saccharomyces cerevisiae* wild-type INVSc1 strain (*MATa his3-D1 leu2 trp1-289 ura3-52*) cells were transformed with the different combinations and grown on minimal medium agar plates lacking corresponding amino acid as indicated in Supplemental Table 5 and Supplemental Figure 1 online.

Cloning and Transgenic Plants

Stable transgenic plants were obtained as previously described (Bourdenx et al., 2011). Mutated *CER1* open reading frames were cloned into the pDONR221 ENTRY vector by Gateway recombinational cloning technology and were subsequently transferred into the pH7WG2D destination vector (Karimi et al., 2002). *Arabidopsis* transient cotransformations were performed as previously described (Marion et al., 2008) with minor modifications. *CER1*, *CYTB5-B*, *CYTB5-C*, *CYTB5-D*, and *CYTB5-E* open reading frames were cloned into the pDONR221 ENTRY vector by Gateway recombinational cloning technology and were subsequently transferred into the pK7WGF2 (*CER1*) or pK7WGY2 (*CYTB5*s) destination vectors (Karimi et al., 2002).

Confocal Analysis

Arabidopsis thaliana cotyledons were transiently cotransformed with GFP-CER1 and YFP-CYTB5 as described above. Colocalization analyses have been performed as previously described (Chatre et al., 2009).

Gene Expression Analysis

RNA was extracted from *Arabidopsis* leaves or yeast cells using the RNeasy Plant Mini Kit (Qiagen). Purified RNA was treated with DNase I using the DNA-free kit (Ambion). For plant tissues, first-strand cDNA was prepared from 10 μg of total RNA with the SuperScript RT II kit (Invitrogen) and oligo$(dT)_{18}$ according to the manufacturer's instructions. For yeast cells, first-strand cDNA was prepared from 63 ng of total RNA with the SuperScript RT II kit (Invitrogen) and random primers according to the manufacturer's instructions. A 1-μL aliquot of the total reaction volume (20 μL) was used as a template in RT-PCR amplification. The PCR amplification was performed with the gene-specific primers listed in Supplemental Table 4 online.

Lipid Analyses

Plant cuticular wax analyses were performed as previously described (Bourdenx et al., 2011). For fatty acyl chain analyses of individual yeast transformants, all transgenic yeasts were grown in 5 to 10 mL of appropriate liquid minimal medium (see Supplemental Table 5 online) supplemented with 2% Gal to induce expression of *Arabidopsis* transgenes (see Supplemental Figure 1D online). Starting from precultures with an OD_{600} of ~0.017, expression cultures were grown for 4 to 6 d at 30°C. Yeast cells of 5 to 10 mL cultures were pelleted and washed in 2 mL NaCl (2.5%, w/v) before fatty acyl chain analyses. FAMEs were obtained by transmethylation at 85°C for 1 h 20 min of yeast cell sediments with 1 mL 0.5 M sulfuric acid in methanol containing 2% v/v dimethoxypropane and 50 μg of heptadecanoic acid (C17:0) as well as 10 μg of docosane (C22 alkane) as internal standards. After cooling, 1 mL NaCl 2.5% (w/v) was added, and fatty acyl chains, including alkanes, were extracted in 1 mL hexane. Extracts were washed with 1 mL 250 mM Tris, pH 8, in NaCl 0.9% (w/v) and then dried under a gentle stream of nitrogen. Samples were dissolved in 200 μL hexane and analyzed by GC-MS as previously described (Domergue et al., 2010). For TLC analysis, ~2000 OD_{600} units were used to prepare FAMEs. The alkane fraction was separated from the extracts by TLC on silica gel plates (20 × 20 cm; Merck) using hexane as the mobile phase then scraped off and extracted in chloroform, concentrated, and analyzed on GC-FID and subsequent GC-MS as previously described (Domergue et al., 2010). For acyl-CoA composition analyses, one OD_{600} unit of transgenic yeasts was collected and used for acyl-CoA extraction and profiling as described (Larson and Graham, 2001).

Interaction Analyses

Split ubiquitin analysis was performed using the yeast two-hybrid system from DUALmembrane system (Dualsystems Biotech AG). The cDNA library was constructed following the manufacturer's instructions (Evrogen) using 660 ng total RNA of epidermis peeled from *Arabidopsis* stems. The library had a complexity of 3.48×10^6 independent clones. For screening, 28 μg of the NubG-cDNA library was used for transformation of THY.AP4 yeast strain (*MATa ura3 leu2 lexA-lacZ-TRP1 lexA-HIS3 lexA-ADE2*) previously transformed with pBT3N:CER1. Yeast transformation efficiency was 1.25×10^5 clones/μg DNA, which indicates whole coverage of the library. Interactors were selected on −HTL medium supplemented with 0.8 mM 3-amino-1,2,4-triazole (Sigma-Aldrich) with further selection on −AHTL and were tested for β-galactosidase activity. For targeted analysis, *CER1*, *CER3*, and *CYTB5s* cDNA were amplified by PCR using *Sfi*I restriction site–containing primers (see Supplemental Table 4 online) with subsequent orientated cloning of *CER1* into pBT3N bait vector and *CER1*, *CER3*, and *CYTB5s* into pPR3N prey vector. THY.AP4 cells were cotransformed with pBT3N:CER1 and pPR3N:PREY or pPR3N empty vector as a negative control. Transformants were selected on −TL, and interactions were assayed on −HTL supplemented with 0.8 mM 3-amino-1,2,4-triazole and −AHTL. To measure β-galactosidase activity of lacZ with X-Gal, cells were grown on −TL and then covered with X-Gal–agarose buffer (0.5% agarose, 0.5 M phosphate buffer, pH 7.0, 0.002% X-Gal) and incubated at 37°C for 10 to 20 min. Split-luciferase analysis was performed as previously described (Van Leene et al., 2010). *CER1*, *CER3*, and *CYTB5s* open reading frames were cloned into the pDONR221 ENTRY vector by Gateway recombination cloning technology using primers detailed in Supplemental Table 4 online. *DPL1* and *SUR2* cloned in the pDONR221 were used as previously described (Marion et al., 2008). Open reading frames were subsequently transferred into appropriate destination vectors (Van Leene et al., 2010).

Accession Numbers

Sequence data from this article can be found in the Arabidopsis Genome Initiative or GenBank/EMBL databases under the following accession numbers: *CER1*, At1g02205; *CER3*, At5g57800; *Actin2*, At1g49240; *CYTB5-B*, At2g32720; *CYTB5-C*, At2g46650; *CYTB5-D*, At5g48810; *CYTB5-E*, At5g53560; *LACS1*, At2g47240; *ACT1*, YFL039C; *At-DPL1*, At1g27980; *At-SUR2B*, At1g14290.

Supplemental Data

The following materials are available in the online version of this article.

Supplemental Figure 1. FAME and Fatty Acyl-CoA Profiles of INVSur4# Yeast Cotransformed with *Arabidopsis* Transgene(s) *CER1* and/or *CER3* and/or *CYTB5-B* and/or *LACS1* and/or Empty Vectors.

Supplemental Figure 2. Identification by GC-MS of the Different Alkanes Produced in the Transgenic INVSur4# Yeast Strain That Coexpressed *Arabidopsis* CER1, CER3, CYTB5-B, and LACS1.

Supplemental Figure 3. FAME Profiles of INVSur4# Cotransformed with CER3, CYTB5, and Wild-Type CER1 or CER1 His Mutants.

Supplemental Figure 4. Cuticular Wax Composition of Inflorescence Stems of *Arabidopsis* Col-0 (Wild-Type), *cer1-1*, *cer1-1*:*CER1*, *cer1-1*:*CER1H146A*, and *cer1-1*:*CER1H248A* Lines.

Supplemental Figure 5. Cuticular Wax Composition of Rosette Leaves of *Arabidopsis* Col-0 (Wild-Type), *cer1-1*, *cer1-1*:*CER1*, *cer1-1*:*CER1H146A*, and *cer1-1*:*CER1H248A* Lines.

Supplemental Figure 6. FAME Profiles of INVSur4# Yeast Cotransformed with CER1 and Wild-Type CER3 or CER3 His Mutants.

Supplemental Figure 7. Sequence Alignment of *Arabidopsis* CER1, CER3, and Cyanobacterial FAAR.

Supplemental Table 1. Inflorescence Stem Cuticular Wax Composition of *Arabidopsis* Col-0, *cer1-1*, *cer1-1*:*CER1*, *cer1-1*:*CER1H146A*, and *cer1-1*:*CER1H248A*.

Supplemental Table 2. Rosette Leaf Cuticular Wax Composition of *Arabidopsis* Col-0, *cer1-1*, *cer1-1*:*CER1*, *cer1-1*:*CER1H146A*, and *cer1-1*:*CER1H248A*.

Supplemental Table 3. Primers Used for Site-Directed Mutagenesis.

Supplemental Table 4. Yeast Expression Vectors and Primers Used for Cloning and PCR Analyses.

Supplemental Table 5. Transgenic Yeasts.

ACKNOWLEDGMENTS

We thank Owen Rowland of Carleton University, Canada, for vectors and stimulating discussions. We thank Su Melser of University of Bordeaux, France, for critical reviews of the article. We also thank Vladimir Denic of Harvard University for providing the p416 MET25-FLAG3:Sur4-F262A/K266L vector. Lipid analyses were carried out at Metabolome facility of Bordeaux (http://www.cgfb.u-bordeaux2.fr/en/metabolome). This study was funded by the Ministère de l'Enseignement Supérieur et de la Recherche (France) (doctoral fellowship for A.B.). This study received support from the Centre National de la Recherche Scientifique and the University Bordeaux Segalen. Rothamsted Research received grant-aided support from the Biotechnology and Biological Sciences Research Council. R.J. was supported by the Canada Research Chairs program, the Natural Sciences and Engineering Council, Canada, and the France-Canada Research Fund.

AUTHOR CONTRIBUTIONS

A.B., F.D., R.J., R.L., and J.J. designed research; A.B., F.D., S.P., and J.J. performed research; C.R., J.-D.F., R.P.H., and J.A.N. contributed analytic tools; A.B., F.D., and J.J. analyzed data; A.B., F.D., R.J., and J.J. wrote the article.

Received April 23, 2012; revised June 5, 2012; accepted June 15, 2012; published July 6, 2012.

REFERENCES

Aarts, M.G., Keijzer, C.J., Stiekema, W.J., and Pereira, A. (1995). Molecular characterization of the *CER1* gene of *Arabidopsis* involved in epicuticular wax biosynthesis and pollen fertility. Plant Cell **7:** 2115–2127.

Bach, L., et al. (2008). The very-long-chain hydroxy fatty acyl-CoA dehydratase PASTICCINO2 is essential and limiting for plant development. Proc. Natl. Acad. Sci. USA **105:** 14727–14731.

Beaudoin, F., Wu, X., Li, F., Haslam, R.P., Markham, J.E., Zheng, H., Napier, J.A., and Kunst, L. (2009). Functional characterization of the Arabidopsis β-ketoacyl-coenzyme A reductase candidates of the fatty acid elongase. Plant Physiol. **150:** 1174–1191.

Bourdenx, B., Bernard, A., Domergue, F., Pascal, S., Léger, A., Roby, D., Pervent, M., Vile, D., Haslam, R.P., Napier, J.A., Lessire, R., and Joubès, J. (2011). Overexpression of Arabidopsis *ECERIFERUM1* promotes wax very-long-chain alkane biosynthesis and influences plant response to biotic and abiotic stresses. Plant Physiol. **156:** 29–45.

Buschhaus, C., and Jetter, R. (2011). Composition differences between epicuticular and intracuticular wax substructures: How do plants seal their epidermal surfaces? J. Exp. Bot. **62:** 841–853.

Chatre, L., Wattelet-Boyer, V., Melser, S., Maneta-Peyret, L., Brandizzi, F., and Moreau, P. (2009). A novel di-acidic motif facilitates ER export of the syntaxin SYP31. J. Exp. Bot. **60:** 3157–3165.

Cheesbrough, T.M., and Kolattukudy, P.E. (1984). Alkane biosynthesis by decarbonylation of aldehydes catalyzed by a particulate preparation from *Pisum sativum*. Proc. Natl. Acad. Sci. USA **81:** 6613–6617.

Chen, X., Goodwin, S.M., Boroff, V.L., Liu, X., and Jenks, M.A. (2003). Cloning and characterization of the *WAX2* gene of *Arabidopsis* involved in cuticle membrane and wax production. Plant Cell **15:** 1170–1185.

Das, D., Eser, B.E., Han, J., Sciore, A., and Marsh, E.N. (2011). Oxygen-independent decarbonylation of aldehydes by cyanobacterial aldehyde decarbonylase: A new reaction of diiron enzymes. Angew. Chem. Int. Ed. Engl. **50:** 7148–7152.

Denic, V., and Weissman, J.S. (2007). A molecular caliper mechanism for determining very long-chain fatty acid length. Cell **130:** 663–677.

Dennis, M.W., and Kolattukudy, P.E. (1991). Alkane biosynthesis by decarbonylation of aldehyde catalyzed by a microsomal preparation from *Botryococcus braunii*. Arch. Biochem. Biophys. **287:** 268–275.

Domergue, F., Vishwanath, S.J., Joubès, J., Ono, J., Lee, J.A., Bourdon, M., Alhattab, R., Lowe, C., Pascal, S., Lessire, R., and Rowland, O. (2010). Three Arabidopsis fatty acyl-coenzyme A reductases, FAR1, FAR4, and FAR5, generate primary fatty alcohols associated with suberin deposition. Plant Physiol. **153:** 1539–1554.

Domínguez, E., Heredia-Guerrero, J.A., and Heredia, A. (2011). The biophysical design of plant cuticles: An overview. New Phytol. **189:** 938–949.

Hwang, Y.T., Pelitire, S.M., Henderson, M.P., Andrews, D.W., Dyer, J.M., and Mullen, R.T. (2004). Novel targeting signals mediate the sorting of different isoforms of the tail-anchored membrane protein cytochrome b5 to either endoplasmic reticulum or mitochondria. Plant Cell **16:** 3002–3019.

Idkowiak-Baldys, J., Takemoto, J.Y., and Grilley, M.M. (2003). Structure-function studies of yeast C-4 sphingolipid long chain base hydroxylase. Biochim. Biophys. Acta **1618:** 17–24.

Javelle, M., Vernoud, V., Rogowsky, P.M., and Ingram, G.C. (2011). Epidermis: The formation and functions of a fundamental plant tissue. New Phytol. **189:** 17–39.

Jeffree, C.E. (1996). Structure and ontogeny of plant cuticles. In Plant Cuticles: An Integrated Functional Approach, G. Kerstiens, ed (Oxford, UK: BIOS Scientific Publishers), pp. 33–82.

Jenks, M.A., Tuttle, H.A., Eigenbrode, S.D., and Feldmann, K.A. (1995). Leaf epicuticular waxes of the *Eceriferum* mutants in Arabidopsis. Plant Physiol. **108:** 369–377.

Jetter, R., and Kunst, L. (2008). Plant surface lipid biosynthetic pathways and their utility for metabolic engineering of waxes and hydrocarbon biofuels. Plant J. **54:** 670–683.

Joubès, J., Raffaele, S., Bourdenx, B., Garcia, C., Laroche-Traineau, J., Moreau, P., Domergue, F., and Lessire, R. (2008).

The VLCFA elongase gene family in *Arabidopsis thaliana*: Phylogenetic analysis, 3D modelling and expression profiling. Plant Mol. Biol. **67:** 547–566.

Joyce, B.L., and Stewart, C.N. Jr. (2011). Designing the perfect plant feedstock for biofuel production: Using the whole buffalo to diversify fuels and products. Biotechnol. Adv., doi/.10.1016/j.biotechadv.2011.08.006

Kamigaki, A., Kondo, M., Mano, S., Hayashi, M., and Nishimura, M. (2009). Suppression of peroxisome biogenesis factor 10 reduces cuticular wax accumulation by disrupting the ER network in *Arabidopsis thaliana*. Plant Cell Physiol. **50:** 2034–2046.

Karimi, M., Inzé, D., and Depicker, A. (2002). GATEWAY vectors for *Agrobacterium*-mediated plant transformation. Trends Plant Sci. **7:** 193–195.

Koornneef, M., Hanhart, C.J., and Thiel, F. (1989). A genetic and phenotypic description of *Eceriferum* (*cer*) mutants in *Arabidopsis thaliana*. J. Hered. **80:** 118–122.

Kosma, D.K., Bourdenx, B., Bernard, A., Parsons, E.P., Lü, S., Joubès, J., and Jenks, M.A. (2009). The impact of water deficiency on leaf cuticle lipids of *Arabidopsis*. Plant Physiol. **151:** 1918–1929.

Kunst, L., and Samuels, L. (2009). Plant cuticles shine: Advances in wax biosynthesis and export. Curr. Opin. Plant Biol. **12:** 721–727.

Kurata, T., Kawabata-Awai, C., Sakuradani, E., Shimizu, S., Okada, K., and Wada, T. (2003). The *YORE-YORE* gene regulates multiple aspects of epidermal cell differentiation in *Arabidopsis*. Plant J. **36:** 55–66.

Larson, T.R., and Graham, I.A. (2001). Technical advance: A novel technique for the sensitive quantification of acyl CoA esters from plant tissues. Plant J. **25:** 115–125.

Li, F., Wu, X., Lam, P., Bird, D., Zheng, H., Samuels, L., Jetter, R., and Kunst, L. (2008). Identification of the wax ester synthase/acyl-coenzyme A: Diacylglycerol acyltransferase WSD1 required for stem wax ester biosynthesis in Arabidopsis. Plant Physiol. **148:** 97–107.

Li, N., Nørgaard, H., Warui, D.M., Booker, S.J., Krebs, C., and Bollinger, J.M., Jr. (2011). Conversion of fatty aldehydes to alka(e)nes and formate by a cyanobacterial aldehyde decarbonylase: Cryptic redox by an unusual dimetal oxygenase. J. Am. Chem. Soc. **133:** 6158–6161.

Li, Y., and Beisson, F. (2009). The biosynthesis of cutin and suberin as an alternative source of enzymes for the production of bio-based chemicals and materials. Biochimie **91:** 685–691.

Lü, S., Song, T., Kosma, D.K., Parsons, E.P., Rowland, O., and Jenks, M.A. (2009). Arabidopsis *CER8* encodes LONG-CHAIN ACYL-COA SYNTHETASE 1 (LACS1) that has overlapping functions with LACS2 in plant wax and cutin synthesis. Plant J. **59:** 553–564.

Maggio, C., Barbante, A., Ferro, F., Frigerio, L., and Pedrazzini, E. (2007). Intracellular sorting of the tail-anchored protein cytochrome b5 in plants: A comparative study using different isoforms from rabbit and *Arabidopsis*. J. Exp. Bot. **58:** 1365–1379.

Marion, J., Bach, L., Bellec, Y., Meyer, C., Gissot, L., and Faure, J. D. (2008). Systematic analysis of protein subcellular localization and interaction using high-throughput transient transformation of *Arabidopsis* seedlings. Plant J. **56:** 169–179.

Nagano, M., Ihara-Ohori, Y., Imai, H., Inada, N., Fujimoto, M., Tsutsumi, N., Uchimiya, H., and Kawai-Yamada, M. (2009). Functional association of cell death suppressor, *Arabidopsis* Bax inhibitor-1, with fatty acid 2-hydroxylation through cytochrome b_5. Plant J. **58:** 122–134.

Pollard, M., Beisson, F., Li, Y., and Ohlrogge, J.B. (2008). Building lipid barriers: Biosynthesis of cutin and suberin. Trends Plant Sci. **13:** 236–246.

Reed, J.R., Vanderwel, D., Choi, S., Pomonis, J.G., Reitz, R.C., and Blomquist, G.J. (1994). Unusual mechanism of hydrocarbon formation in the housefly: Cytochrome P450 converts aldehyde to the sex pheromone component (Z)-9-tricosene and CO_2. Proc. Natl. Acad. Sci. USA **91:** 10000–10004.

Rowland, O., Lee, R., Franke, R., Schreiber, L., and Kunst, L. (2007). The *CER3* wax biosynthetic gene from *Arabidopsis thaliana* is allelic to *WAX2/YRE/FLP1*. FEBS Lett. **581:** 3538–3544.

Rowland, O., Zheng, H., Hepworth, S.R., Lam, P., Jetter, R., and Kunst, L. (2006). *CER4* encodes an alcohol-forming fatty acyl-coenzyme A reductase involved in cuticular wax production in *Arabidopsis*. Plant Physiol. **142:** 866–877.

Samuels, L., Kunst, L., and Jetter, R. (2008). Sealing plant surfaces: Cuticular wax formation by epidermal cells. Annu. Rev. Plant Biol. **59:** 683–707.

Schirmer, A., Rude, M.A., Li, X., Popova, E., and del Cardayre, S.B. (2010). Microbial biosynthesis of alkanes. Science **329:** 559–562.

Schneider-Belhaddad, F., and Kolattukudy, P. (2000). Solubilization, partial purification, and characterization of a fatty aldehyde decarbonylase from a higher plant, *Pisum sativum*. Arch. Biochem. Biophys. **377:** 341–349.

Shanklin, J., Achim, C., Schmidt, H., Fox, B.G., and Münck, E. (1997). Mössbauer studies of alkane omega-hydroxylase: Evidence for a diiron cluster in an integral-membrane enzyme. Proc. Natl. Acad. Sci. USA **94:** 2981–2986.

Shanklin, J., and Cahoon, E.B. (1998). Desaturation and related modifications of fatty acids. Annu. Rev. Plant Physiol. Plant Mol. Biol. **49:** 611–641.

Shepherd, T., and Wynne Griffiths, D. (2006). The effects of stress on plant cuticular waxes. New Phytol. **171:** 469–499.

Sperling, P., Ternes, P., Zank, T.K., and Heinz, E. (2003). The evolution of desaturases. Prostaglandins Leukot. Essent. Fatty Acids **68:** 73–95.

Sturaro, M., Hartings, H., Schmelzer, E., Velasco, R., Salamini, F., and Motto, M. (2005). Cloning and characterization of *GLOSSY1*, a maize gene involved in cuticle membrane and wax production. Plant Physiol. **138:** 478–489.

Taton, M., Husselstein, T., Benveniste, P., and Rahier, A. (2000). Role of highly conserved residues in the reaction catalyzed by recombinant Delta7-sterol-C5(6)-desaturase studied by site-directed mutagenesis. Biochemistry **39:** 701–711.

Van Leene, J., et al. (2010). Targeted interactomics reveals a complex core cell cycle machinery in *Arabidopsis thaliana*. Mol. Syst. Biol. **6:** 397.

Vioque, J., and Kolattukudy, P.E. (1997). Resolution and purification of an aldehyde-generating and an alcohol-generating fatty acyl-CoA reductase from pea leaves (*Pisum sativum* L.). Arch. Biochem. Biophys. **340:** 64–72.

Zheng, H., Rowland, O., and Kunst, L. (2005). Disruptions of the *Arabidopsis* Enoyl-CoA reductase gene reveal an essential role for very-long-chain fatty acid synthesis in cell expansion during plant morphogenesis. Plant Cell **17:** 1467–1481.

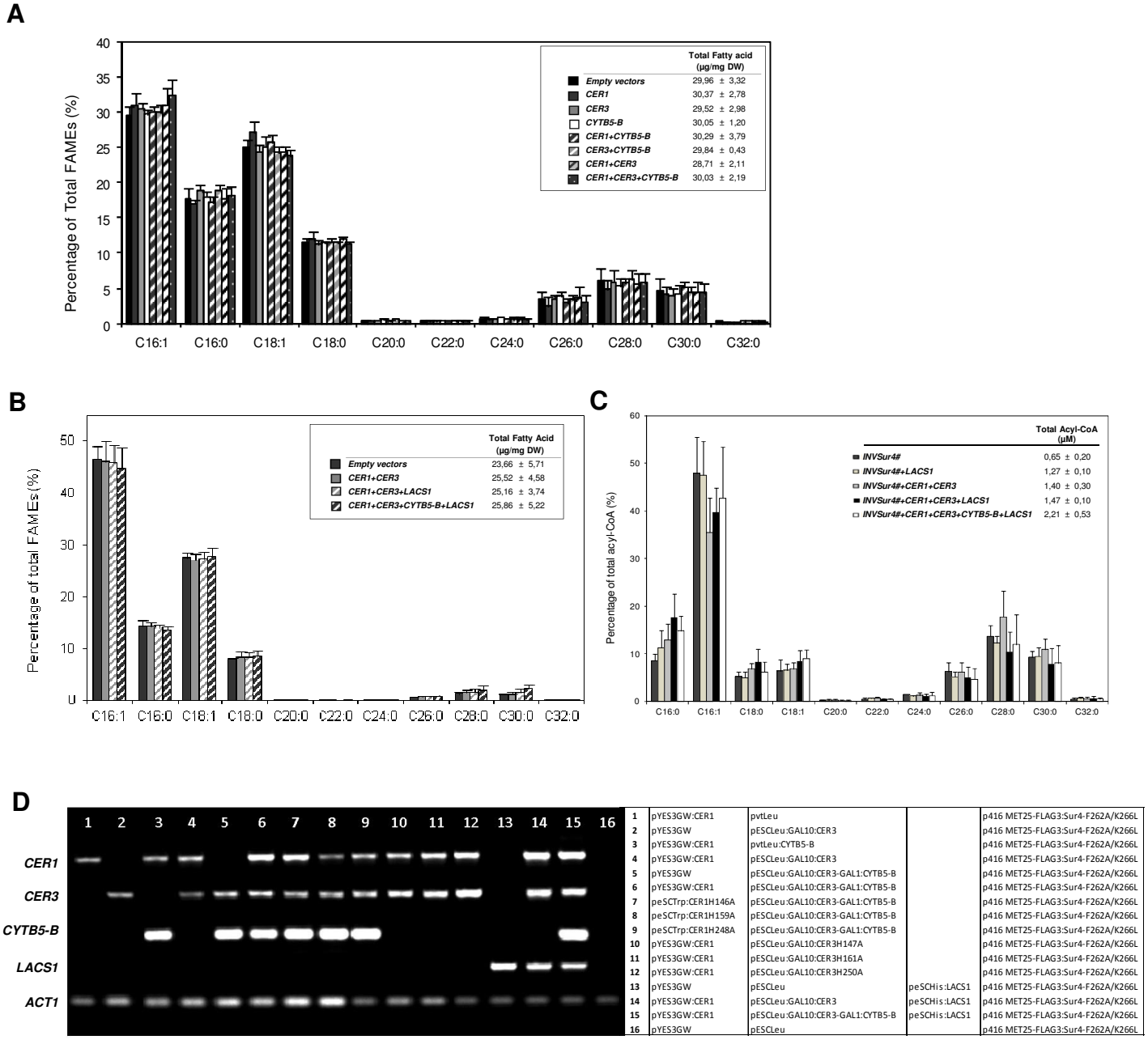

1	pYES3GW:CER1	pvtLeu		p416 MET25-FLAG3:Sur4-F262A/K266L
2	pYES3GW	pESCLeu:GAL10:CER3		p416 MET25-FLAG3:Sur4-F262A/K266L
3	pYES3GW:CER1	pvtLeu:CYTB5-B		p416 MET25-FLAG3:Sur4-F262A/K266L
4	pYES3GW:CER1	pESCLeu:GAL10:CER3		p416 MET25-FLAG3:Sur4-F262A/K266L
5	pYES3GW	pESCLeu:GAL10:CER3-GAL1:CYTB5-B		p416 MET25-FLAG3:Sur4-F262A/K266L
6	pYES3GW:CER1	pESCLeu:GAL10:CER3-GAL1:CYTB5-B		p416 MET25-FLAG3:Sur4-F262A/K266L
7	peSCTrp:CER1H146A	pESCLeu:GAL10:CER3-GAL1:CYTB5-B		p416 MET25-FLAG3:Sur4-F262A/K266L
8	peSCTrp:CER1H159A	pESCLeu:GAL10:CER3-GAL1:CYTB5-B		p416 MET25-FLAG3:Sur4-F262A/K266L
9	peSCTrp:CER1H248A	pESCLeu:GAL10:CER3-GAL1:CYTB5-B		p416 MET25-FLAG3:Sur4-F262A/K266L
10	pYES3GW:CER1	pESCLeu:GAL10:CER3H147A		p416 MET25-FLAG3:Sur4-F262A/K266L
11	pYES3GW:CER1	pESCLeu:GAL10:CER3H161A		p416 MET25-FLAG3:Sur4-F262A/K266L
12	pYES3GW:CER1	pESCLeu:GAL10:CER3H250A		p416 MET25-FLAG3:Sur4-F262A/K266L
13	pYES3GW	pESCLeu	peSCHis:LACS1	p416 MET25-FLAG3:Sur4-F262A/K266L
14	pYES3GW:CER1	pESCLeu:GAL10:CER3	peSCHis:LACS1	p416 MET25-FLAG3:Sur4-F262A/K266L
15	pYES3GW:CER1	pESCLeu:GAL10:CER3-GAL1:CYTB5-B	peSCHis:LACS1	p416 MET25-FLAG3:Sur4-F262A/K266L
16	pYES3GW	pESCLeu		p416 MET25-FLAG3:Sur4-F262A/K266L

Supplemental Figure 1. Fatty acyl methyl ester and fatty acyl-CoA profiles of INVSur4# yeast co-transformed with Arabidopsis transgene(s) *CER1* and/or *CER3* and/or *CYTB5-B* and/or *LACS1* and/or empty vectors. **(A and B)** Comparison of the FAME profile of INVSur4# control yeast (transformed with empty vectors) with the FAME profiles of INVSur4# yeasts transformed with Arabidopsis transgenes as detailed in the legend. Mean values (%) of percentage of total FAMEs are given with SD. Quantifications of total fatty acids in INVSur4# control yeast (transformed with empty vectors) compared to INVSur4# yeasts transformed with Arabidopsis transgenes as detailed in the legends correspond to mean values (µg/mg of dry weight (DW)) of total fatty acids as FAMEs given with SD. **(A)** Yeast were grown in SC-TLU (3≤n≤17). **(B)** Yeast were grown in SD-HTLU (6≤n≤8). (**C)** Comparison of the acyl-CoA profile of INVSur4# control yeast (transformed with empty vectors) with the acyl-CoA profiles of INVSur4# yeasts transformed with Arabidopsis transgenes as detailed in the legend. Mean values (%) of percentage of total acyl-CoAs are given with SD (n=5). Quantifications of total acyl-CoA in INVSur4# control yeast (transformed with empty vectors) compared to INVSur4# yeasts transformed with Arabidopsis transgenes as detailed in the legends correspond to mean values (µM) given with SD (n=5) (**D)** RT-PCR analysis of steady-state *CER1*, *CER3*, *CYTB5-B* and *LACS1* transcripts in INVSc1 transformed with constructs indicated in the table. The yeast *Actin1* (*ACT1*) gene was used as a constitutively expressed control.

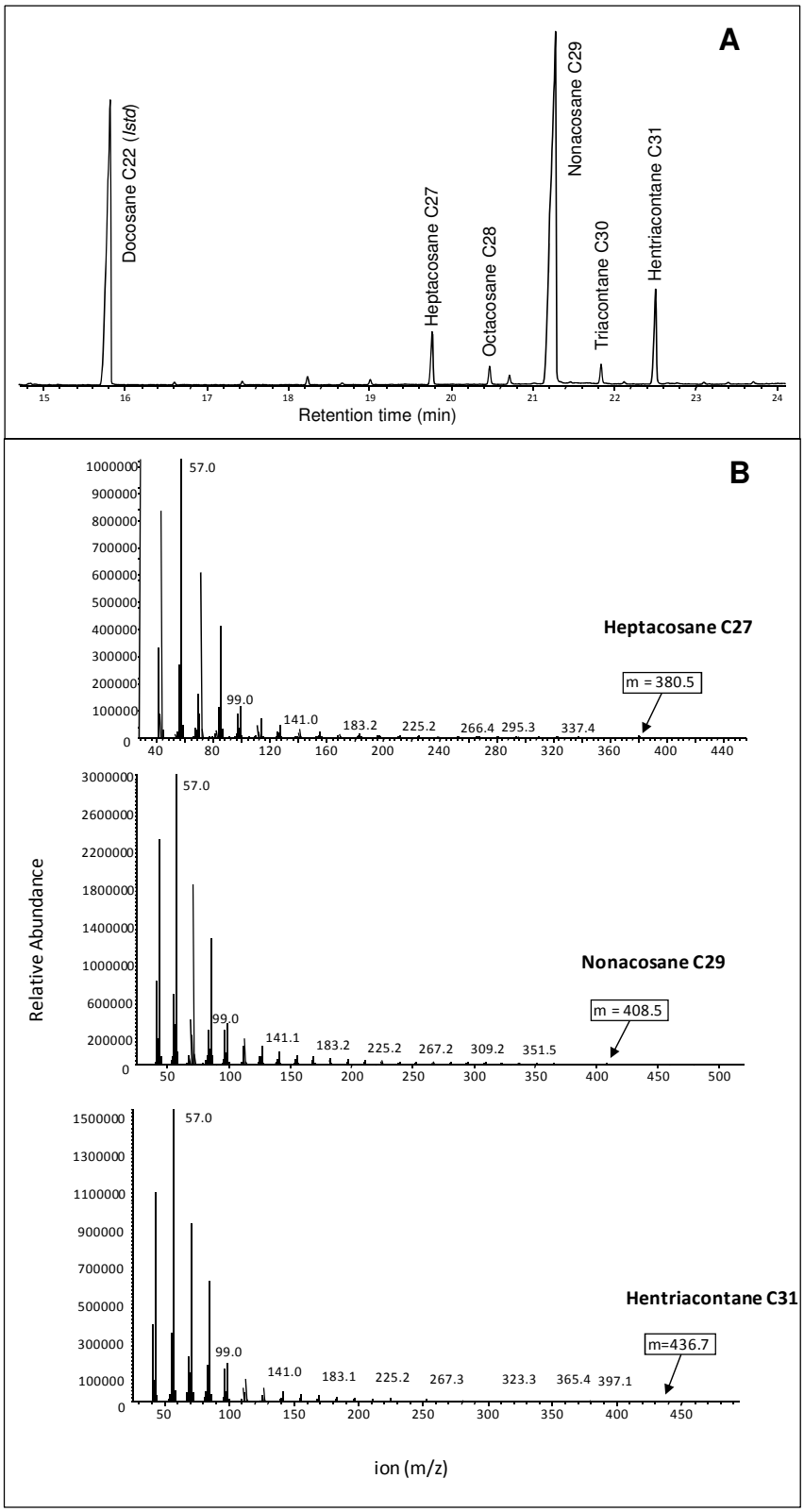

Supplemental Figure 2. Identification by GC-MS of the different alkanes produced in the transgenic INVSur4# yeast strain that co-expressed Arabidopsis CER1, CER3, CYTB5-B and LACS1. **(A)** GC-MS trace of hydrocarbon fraction separated from total lipid extract by TLC. Docosane (Alkane C22, 20µg) was used as internal standard. **(B)** Mass spectra of the major alkane peaks indicated in panel A.

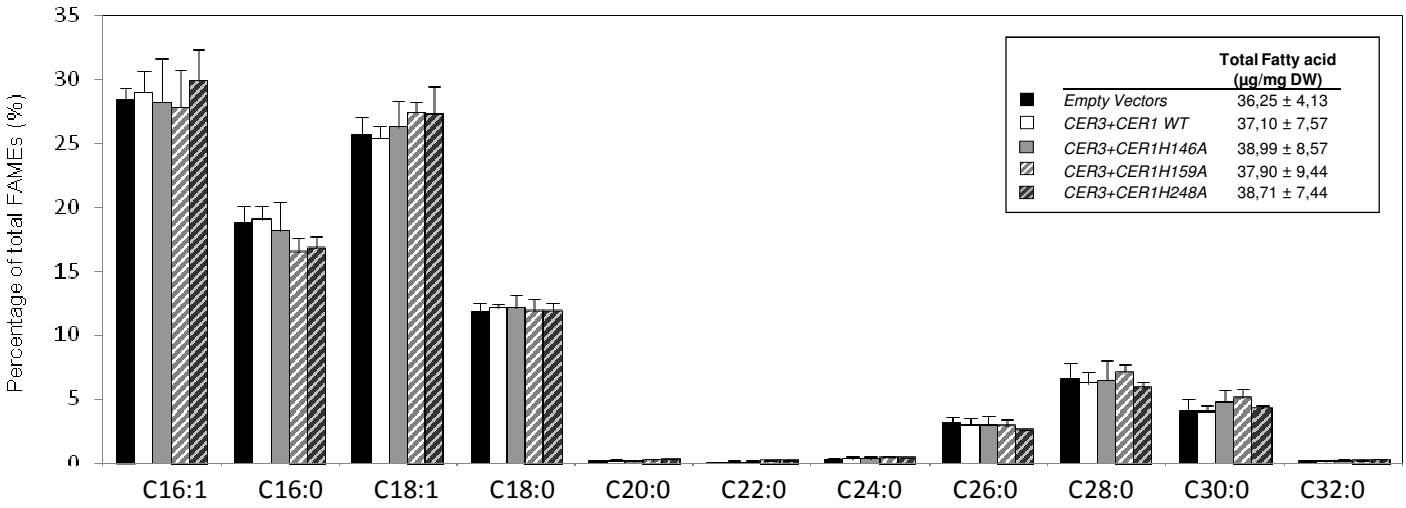

Supplemental Figure 3. Fatty acyl methyl ester profiles of INVSur4# co-transformed with CER3, CYTB5 and wild-type CER1 or CER1 histidine mutants.

Comparison of the FAME profile of INVSur4# control yeast (transformed with empty vectors) with the FAME profiles of INVSur4# yeasts transformed with Arabidopsis transgenes as detailed in the legend. Mean values (%) of percentage of total FAMEs are given with SD ($6 \leq n \leq 17$). Quantification of total FAMEs in INVSur4# control yeast (transformed with empty vectors) compared to INVSur4# yeast transformed with Arabidopsis transgenes as detailed in the legend. Mean values (µg/mg of dry weight (DW)) of total fatty acids as FAMEs are given with SD ($3 \leq n \leq 14$)

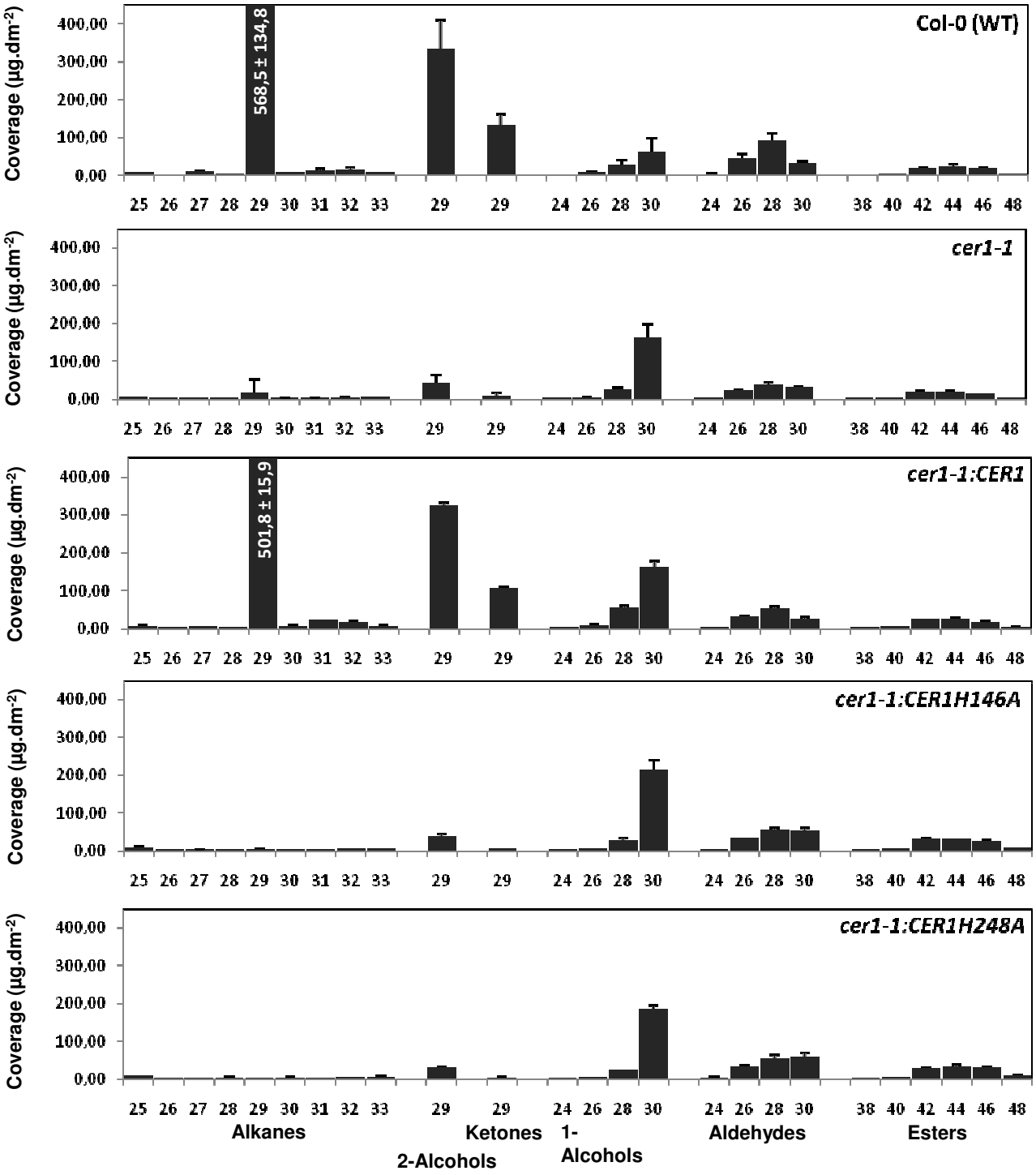

Supplemental Figure 4. Cuticular wax composition of inflorescence stems of Arabidopsis Col-0 (WT), *cer1-1*, *cer1-1:CER1*, *cer1-1:CER1H146A* and *cer1-1:CER1H248A* lines. Wax coverage is expressed as µg.dm^{-2} of stem surface area. Each wax constituent is designated by carbon chain-length and is labelled by chemical class along x-axis. Each value represents the mean ± S.D. (n=3)

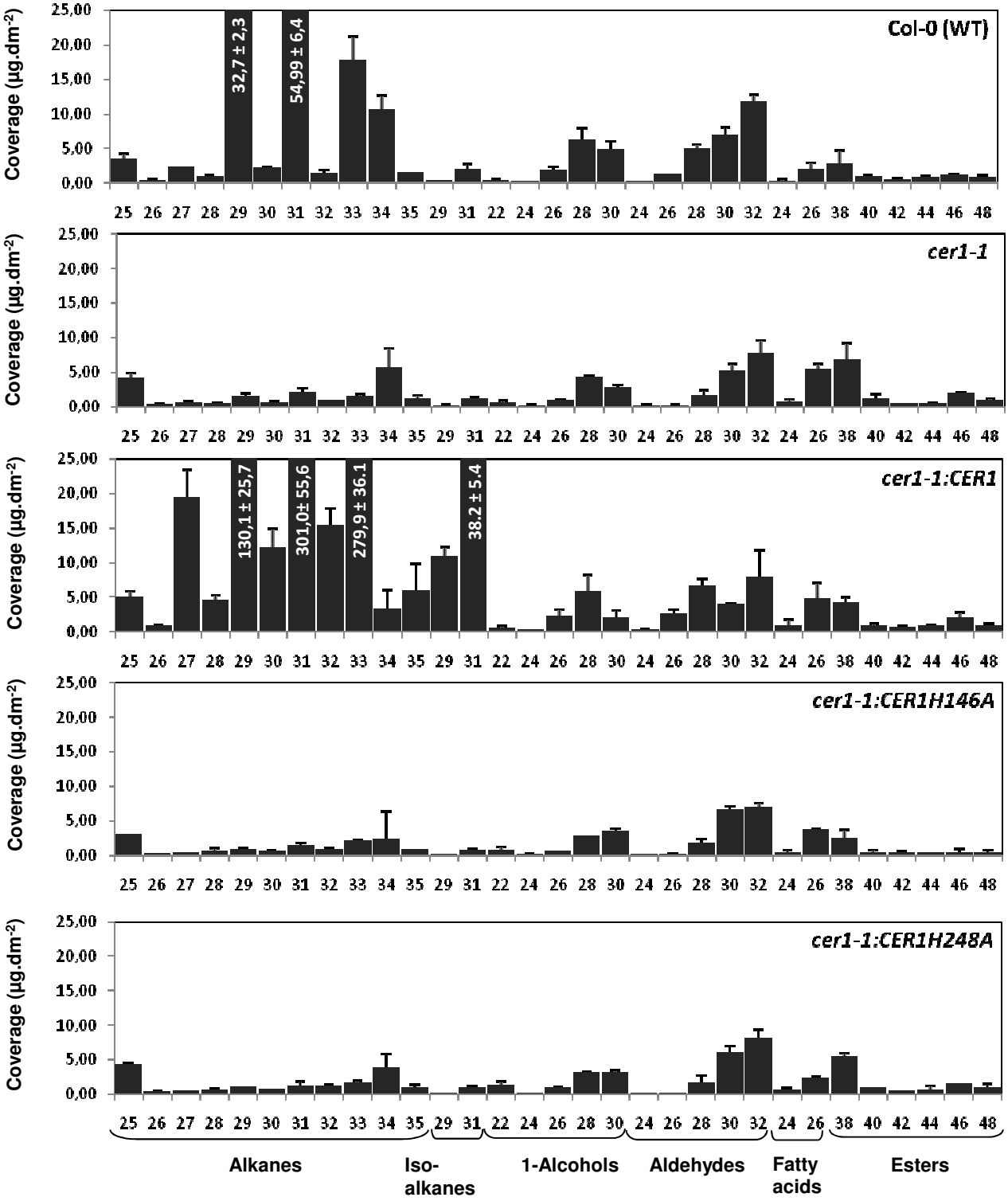

Supplemental Figure 5. Cuticular wax composition of rosette leaves of Arabidopsis Col-0 (WT), *cer1-1*, *cer1-1:CER1*, *cer1-1:CER1H146A* and *cer1-1:CER1H248A* lines. Wax coverage is expressed as µg.dm-² of leaf surface area. Each wax constituent is designated by carbon chain-length and is labelled by chemical class along x-axis. Each value represents the mean ± S.D.(n=3)

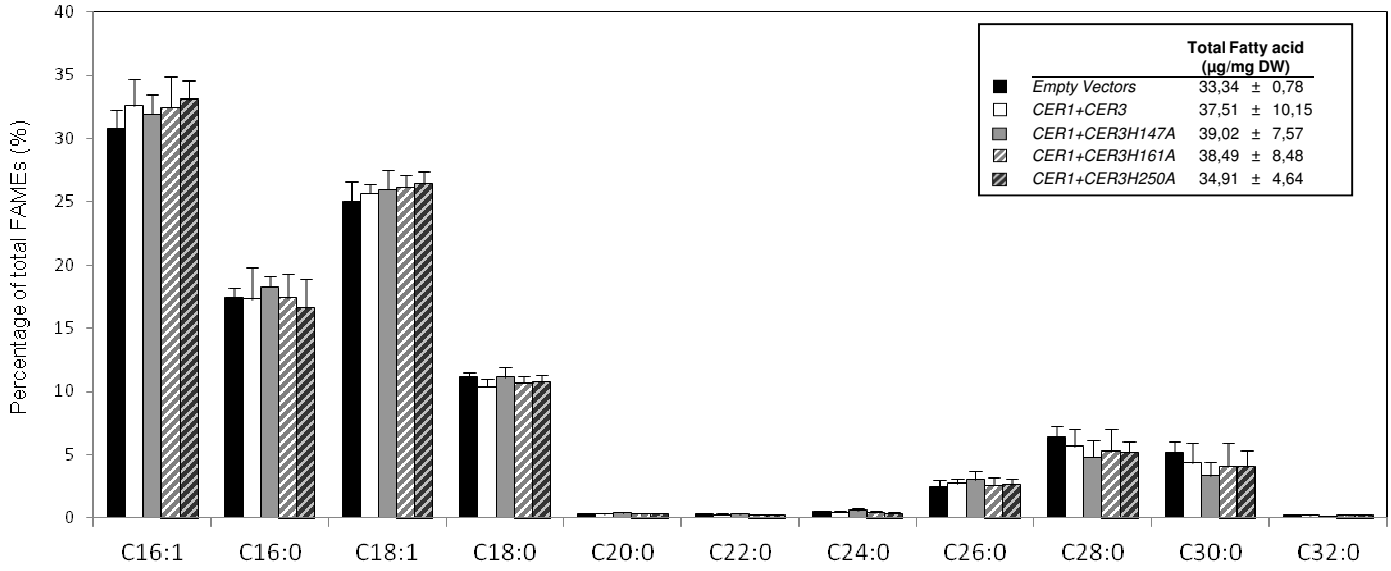

Supplemental Figure 6. Fatty acyl methyl ester profiles of INVSur4# yeast co-transformed with CER1 and wild-type CER3 or CER3 histidine mutants.

Comparison of the FAME profile of INVSur4# control yeast (transformed with empty vectors) with the FAME profiles of INVSur4# yeasts transformed with Arabidopsis transgenes as detailed in the legend. Mean values (%) of percentage of total FAMEs are given with SD (6≤n≤17). Quantification of total FAMEs in INVSur4# control yeast (transformed with empty vectors) compared to INVSur4# yeast transformed with Arabidopsis transgenes as detailed in the legend. Mean values (µg/mg of dry weight (DW)) of total fatty acids as FAMEs are given with SD (3≤n≤14)

A

```
CER1            MATKPGVLTDWPWTPLGSFKYIVIAPWAVHSTYRFVTDDPEKRDLGYFLVFPFLLFRILH 60
CER3            ---MVAFLSAWPWENFGNLKYLLYAPLAAQVVYSWVYEEDISKVLWCIHILIICGLKALV 57
                     ..*: ***  :*.:**:: ** *.: .* :* ::  .: *  : :: :  :: *

CER1            NQVWISLSRYYTSSGKRRIVDKGIDFNQVDRETNWDDQILFN----GVLFYIGINLLPEA 116
CER3            HELWSVFNNMLFVTRTLRINPKGIDFKQIDHEWHWDNYIILQAIIVSLICYMSPPLMMMI 117
                :::*  :..    : . **  *****:*:*:* :**: *:::    .:: *:.  *:

                                          HXXXH          HXXHH
CER1            KQLPWWRTDGVLMAALIHTGPVEFLYYWLHKALHHH-FLYSRYHSHHHSSIVTEPITSVI 175
CER3            NSLPLWNTKGLIALIVLHVTFSEPLYYFLHRSFHRNNYFFTHYHSFHHSSPVPHPMTAGN 177
                :.** *.*.*::   ::*.   * ***:**:::*:: :::::***.**** *..*:*:

CER1            HPFAEHIAYFILFAIPLLTTLLTKTASIISFAGYIIYIDFMNNMGHCNFELIPKRLFHLF 235
CER3            ATLLENIILCVVAGVPLIGCCLFGVGSLSAIYGYAVMFDFMRCLGHCNVEIFSHKLFEIL 237
                 .: *:*   :: .:**:   *  ..*: :: ** : :***. :****.*::.::**.::

                        HXXHH
CER1            PPLKFLCYTPSYHSLHHTQFRTNYSLFMPLYDYIYGTMDESTDTLYEKTLERGDD---IV 292
CER3            PVLRYLIYTPTYHSLHHQEMGTNFCLFMPLFDVLGDTQNPNSWELQKKIRLSAGERKRVP 297
                * *::* ***:****** :: **:.*****:* : .* : .:  * :*    ..:   :

CER1            DVVHLTHLTTPESIYHLRIGLASFASYPFAYRWFMRLLWPFTSLSMIFTLFYARLFVAER 352
CER3            EFVFLAHGVDVMSAMHAPFVFRSFASMPYTTRIFLLPMWPFTFCVMLGMWAWSKTFLFSF 357
                :.*.*:* .   *  *  : : **** *:: * *:  :****   *:    ::: *: .

CER1            NSFNKLNLQSWVIPRYNLQYLLKWRKEAINNMIEKAILEADKKGVKVLSLGLMNQGEELN 412
CER3            YTLRNNLCQTWGVPRFGFQYFLPFATKGINDQIEAAILRADKIGVKVISLAALNKNEALN 417
                 ::.:   *:* :**:.:**:* : .:.**: ** ***.*** ****:**. :*:.* **

CER1            RNGEVYIHNHPDMKVRLVDGSRLAAAVVINSVPKATTSVVMTGNLTKVAYTIASALCQRG 472
CER3            GGGTLFVNKHPDLRVRVVHGNTLTAAVILYEIPKDVNEVFLTGATSKLGRAIALYLCRRG 477
                 .* :::::***::**:*.*. *:***:: .:** ...*.:**  :*:. :**  **:**

CER1            VQVS--TLRLDEYEKIRSCVPQECRDHLVYLTS-EALSSNKVWLVGEGTTREEQEKATKG 529
CER3            VRVLMLTLSMERFQKIQKEAPVEFQNNLVQVTKYNAAQHCKTWIVGKWLTPREQSWAPAG 537
                *:*   ** ::.::**:. .* * :::** :*. :* .  *.*:**:  * .**. *. *

CER1            TLFIPFSQFPLKQLRRDCIYHTTPALIVPKSLVNVHSCENWLPRKAMSATRVAGILHALE 589
CER3            THFHQFVVPPILKFRRNCTYGDLAAMKLPKDVEGLGTCEYTMERGVVHACHAGGVVHMLE 597
                * *  *   *: ::**:* *   .*: :**.: .: :**  : * .: * :..*::* **

CER1            GWEMHECGTSLLLSDLDQVWEACLSHGFQPLLLPHH 625
CER3            GWKHHEVG-AIDVDRIDLVWEAAMKYGLSAVSSLTN 632
                **: ** * :: :. :* ****.:.:*:..:    :
```

B

```
CER1            VVMTGNLTKVAYTIASALCQRGVQVS--TLRLDEYEKIRSCVPQECRDHLVYLTS-EALS 507
CER3            VFLTGATSKLGRAIALYLCRRGVRVLMLTLSMERFQKIQKEAPVEFQNNLVQVTKYNAAQ 515
FAAR            VAVVGATGDIGSAVCRWLDLK-LGVGDLILTARNQERLDNLQAELGRGKILPLEAALPEA 216
                * :.*   .:. ::.  *  : : *    *   . ::: .  .   :.::: :    .

CER1            SNKVWLVGEGT------TREEQEKATKGTLFIPFSQFPLKQLRRDCIYHTTPALIVPKSL 561
CER3            HCKTWIVGKWL------TPREQSWAPAGTHFHQFVVPPILKFRRNCTYGDLAAMKLPKDV 569
FAAR            DFIVWVASMPQGVVIDPATLKQPCVLIDGGYPKNLGSKVQGEGIYVLNGGVVEHCFDIDW 276
                   .*:..         :  :*  .  .  :       :                .  .

CER1            VNVHSCENWLPRKAMSATRVAGILHALEGWEMHECGT--SLLLSDLDQVWEACLSHGFQP 619
CER3            EGLGTCEYTMERGVVHACHAGGVVHMLEGWKHHEVG---AIDVDRIDLVWEAAMKYGLSA 626
FAAR            QIMSAAEMARPERQMFACFAEAMLLEFEGWHTNFSWGRNQITIEKMEAIGEASVRHGFQP 336
                  : :.*    .  : *  . .::  :***. :       : :. :: : **.: :*:..
```

Supplemental Figure 7. Sequence alignment of Arabidopsis CER1, CER3 and cyanobacterial FAAR **(A)** Sequence alignment of Arabidopsis CER1 and CER3. Deduced amino acid sequences of CER1 (At1g02205) and CER3 (At5g57800) were compared using the multiple alignment program CLUSTALW2. Gaps (-) were introduced for maximizing the alignment. The identical residues are represented by stars. The similar residues are represented by colons and dots. Positions of three histidine-rich motifs are indicated in bold. Positions of the long hydrophobic domains are boxed in grey. Position of the WAX2 C-terminal domain (pfam12076) containing the conserved LEGW sequence motif (bold) is boxed in black. **(B)** Sequence alignment of Arabidopsis CER1 and CER3 with the cyanobacterial FAAR. Amino acid sequence alignment of the WAX2 Cterminal domains of Arabidopsis CER1 and CER3 with C-terminal part of the Synechococcus elongatus PCC7942 Fatty Acyl-ACP Reductase (FAAR) (gi, 1399843; gb, AAB82039). Position of the WAX2 C-terminal domain (pfam12076) in the FAAR sequence containing the EGW sequence motif (bold) is boxed in black.

Supplemental Table 1. Inflorescence stems cuticular wax composition of Arabidopsis Col-0, *cer1-1*, *cer1-1:CER1*, *cer1-1:CER1H146A* and *cer1-1:CER1H248A*.

Line	Total load	n-Alkanes	2-Alcohols	Ketones	1-Alcohols	Aldehydes	Esters
Col-0	1444,1 ± 102,0	633,6 ± 51,8	333,4 ± 76,8	134,7 ± 27,2	173,8 ± 21,9	97,5 ± 23,4	71,0 ± 5,4
cer1-1R	1413,3 ± 52,7	571,2 ± 19,7	322,9 ± 7,8	107,0 ± 2,4	109,3 ± 8,2	226,3 ± 14,3	76,6 ± 14,9
cer1-1	445,9 ± 83,4	41,9 ± 10,6	42,8 ± 21,5	8,6 ± 8,3	96,0 ± 5,1	193,1 ± 20,2	63,4 ± 3,0
cer1-1:CER1H146A	578,9 ± 22,4	36,1 ± 1,7	39,0 ± 5,8	6,2 ± 0,9	143,9 ± 7,0	251,0 ± 15,1	102,6 ± 4,0
cer1-1:CER1H248A	544,8 ± 19,0	36,4 ± 3,2	31,4 ± 2,8	4,1 ± 0,4	150,9 ± 13,2	216,6 ± 11,9	105,4 ± 8,5

Mean values (µg.dm^{-2}) of total wax loads and coverage of individual compound classes are given with SD (n=3)

Supplemental Table 2. Rosette leaves cuticular wax composition of Arabidopsis Col-0, *cer1-1*, *cer1-1:CER1*, *cer1-1:CER1H146A* and *cer1-1:CER1H248A*.

Line	Total load	n-Alkanes	Iso-Alkanes	1-Alcohols	Aldehydes	Fatty acids	Esters
Col-0	179,5 ± 16,4	128,7 ± 7,2	2,4 ± 0,5	13,7 ± 1,9	25,2 ± 1,3	2,3 ± 1,1	7,1 ± 1,1
cer1-1R	875,1 ± 91,1	778,0 ± 84,7	49,1 ± 4,6	11,1 ± 2,1	21,4 ± 2,5	5,7 ± 3,2	9,8 ± 1,0
cer1-1	62,6 ± 3,4	19,1 ± 1,7	1,5 ± 0,2	9,0 ± 1,2	14,9 ± 2,3	6,3 ± 1,0	11,8 ± 1,4
cer1-1:CER1H146A	47,8 ± 3,2	13,9 ± 2,2	0,8 ± 0,1	7,9 ± 1,1	16,0 ± 1,8	4,2 ± 0,9	4,9 ± 1,2
cer1-1:CER1H248A	56,4 ± 3,3	16,6 ± 1,4	1,1 ± 0,2	9,0 ± 0,6	16,3 ± 2,1	3,0 ± 0,6	10,2 ± 1,8

Mean values (µg.dm^{-2}) of total wax loads and coverage of individual compound classes are given with SD (n=3)

Supplemental Table 3. Primers used for site-directed mutagenesis

Genes	**Mutations**	**Forward primer (5' 3')**
CER1 (At1g02205)	CER1H146A	TATTATTGGCTC**GCT**AAAGCTCTCCAC
	CER1H159A	TTCCCGCTAC**GCT**TCCCACCACCA
	CER1H248A	ACCCCCTCATAC**GCT**TCGCTGCACCAC
CER3 (At5g57800)	CER3H147A	TACTTTCTG**GCT**AGATCTTTCCATCGTAAC
	CER3H161A	TTCACACATTAC**GCT**TCTTTCCACCACTCA
	CER3H250A	ACTCCAACGTAC**GCT**AGTCTGCATCAT

Supplemental Table 4. Yeast expression vectors and primers used for cloning and PCR analyses.

Genes	*ID*	Forward primer (5' 3')	Reverse primer (5' 3')	Yeast expression vectors
Primers used for gateway cloning of cDNAs or histidine mutated cDNAs				
CER1	*At1g02205*	GGGGACAAGTTTGTACAAAAAAGCAGGCTTAATGGCCACAAAACCAGGAGTCCTCACC	AGAAAGCTGGGTCTAATAAATTAGTTGGAT	pYES3GW
CER3	*At5g57800*	GGGGACAAGTTTGTACAAAAAAGCAGGCTTAATGGTTGCTTTTTTATCAGCTTGGCCT	GGGGACCACTTTGTACAAGAAAGCTGGGTGATTTGTGAGTGAAGAAACAGCACT	
CYTB5-B	*At2g32720*	AAAAAGCAGGCTTAATGGGAGACGAAGCAAAGATCTTCACTC	AGAAAGCTGGGTGCTACCCTGATTTGGTGTAGATACGGATTC	pvtLeu
CYTB5-C	*At2g46650*	AAAAAGCAGGCTTAATGGCGAATCTAATTTCGTTTCACGATGTG	AGAAAGCTGGGTGCTACTTGTTGTTGTAGAATCTGAGAGCGAAA	
CYTB5-D	*At5g48810*	AAAAAGCAGGCTTAATGGGCGGAGACGGAAAAGTTTTCAC	AGAAAGCTGGGTGTCAAGAAGAAGGAGCCTTGGTCTTAGTG	
CYTB5-E	*At5g53560*	AAAAAGCAGGCTTAATGTCTTCAGATCGGAAGGTTCTAAGTTTTG	AGAAAGCTGGGTGCTAGTCTTTCTTGGTATAGTGACGGACG	
Primers used for *Sfi* orientated pBT3N or/and pPR3N cloning of cDNAs				
CER1	*At1g02205*	CGCAGAGTGGCCATTACGGCCATGGCCACAAAACCAGGAGTCCTCACC	TCTCGAGAGGCCGAGGCGGCCTTAATGATGTGGAAGGAGGAGAGGCTGGAA	
CER3	*At5g57800*	CGCAGAGTGGCCATTACGGCCATGGTTGCTTTTTTATCAGCTTGGCCTTGG	TCTCGAGAGGCCGAGGCGGCCTCAATTTGTGAGTGAAGAAACAGCACTAAGACC	
CYTB5-B	*At2g32720*	CGCAGAGTGGCCATTACGGCCATGGGAGACGAAGCAAAGATCTTCACTC	TCTCGAGAGGCCGAGGCGGCCCTACCCTGATTTGGTGTAGATACGGATTC	
CYTB5-C	*At2g46650*	CGCAGAGTGGCCATTACGGCCATGGCGAATCTAATTTCGTTTCACGATGT	TCTCGAGAGGCCGAGGCGGCCCTACTTGTTGTTGTAGAATCTGAGAGCGAAA	
CYTB5-D	*At5g48810*	CGCAGAGTGGCCATTACGGCCATGGGCGGAGACGGAAAAGTTTTCAC	TCTCGAGAGGCCGAGGCGGCCTCAAGAAGAAGGAGCCTTGGTCTTAGTG	
CYTB5-E	*At5g53560*	CGCAGAGTGGCCATTACGGCCATGTCTTCAGATCGGAAGGTTCTAAGTTTTG	TCTCGAGAGGCCGAGGCGGCCCTAGTCTTTCTTGGTATAGTGACGGACG	
Primers used for peSC:GAL10 cloning of cDNAs or histidine mutated cDNAs				
CER1	*At1g02205*	CCATCGATACTAGTATGGCCACAAAACCAGGAGTCCTC	TAAGATCTGAGCTCTTAATGATGTGGAAGGAGGAGAGGCTG	pESCTrp
CER3	*At5g57800*	CCATCGATACTAGTATGGTTGCTTTTTTATCAGCTTGGCCTTGG	TAAGATCTGAGCTCTCAATTTGTGAGTGAAGAAACAGCACTAAGA	pESCLeu
LACS1	*At2g47240*	AGAGGATCCATGAAGTCTTTTGCGGCTAAG	AGAGTCGACTCAGATTTTCTTTGAGGCCAAT	pESCHis
Primers used for peSC:GAL1 cloning of cDNAs or histidine mutated cDNAs				
CER1	*At1g02205*	AACCCCGGATCCATGGCCACAAAACCAGGAGTCCTC	AGCTTACTCGAGTTAATGATGTGGAAGGAGGAGAGGCTG	pESCTrp
CYTB5-B	*At2g32720*	AACCCCGGATCCATGGGAGACGAAGCAAAGATCTTCACTC	AGCTTACTCGAGCTACCCTGATTTGGTGTAGATACGGATTC	pESCLeu:GAL10:CER3
Primers used for semi-quantitative PCR analysis in Arabidopsis				
ACT2	*At1g04924*	CCGAGCAGCATGAAGATTAAG	CATACTCTGCCTTAGAGATCCACA	
CER1	*At1g02205*	GCGGGTACCATGGCCACAAAACCAGGAGTC	GCGCTCGAGTCATTAATGATGTGGAAGGAGGAGAGG	
Primers used for semi-quantitative PCR analysis in yeast				
ACT1	*YFL039C*	ACTGAATTAACAATGGATTC	GTAACGTAAAGTCAAGATAC	
CER1	*At1g02205*	AACCCCGGATCCATGGCCACAAAACCAGGAGTCCTC	AGCTTACTCGAGTTAATGATGTGGAAGGAGGAGAGGCTG	
CER3	*At5g57800*	CCATCGATACTAGTATGGTTGCTTTTTTATCAGCTTGGCCTTGG	TAAGATCTGAGCTCTCAATTTGTGAGTGAAGAAACAGCACTAAGA	
CYTB5-B	*At2g32720*	AACCCCGGATCCATGGGAGACGAAGCAAAGATCTTCACTC	AGCTTACTCGAGCTACCCTGATTTGGTGTAGATACGGATTC	
LACS1	*At2g47240*	AGAGGATCCATGAAGTCTTTTGCGGCTAAG	AGAGTCGACTCAGATTTTCTTTGAGGCCAAT	

Supplemental Table 5. Transgenic yeasts

GENES expressed	Expression Vectors				Selection medium
SUR4# + CER1	pYES3GW:CER1	pvtLeu	p416 MET25-FLAG3:Sur4-F262A/K266L		-TRP-LEU-URA
SUR4# + CER3	pYES3GW	pESCLeu:GAL10:CER3	p416 MET25-FLAG3:Sur4-F262A/K266L		-TRP-LEU-URA
SUR4# + CER1+CYTB5-B	pYES3GW:CER1	pvtLeu:CYTB5-B	p416 MET25-FLAG3:Sur4-F262A/K266L		-TRP-LEU-URA
SUR4# + CER1+CER3	pYES3GW:CER1	pESCLeu:GAL10:CER3	p416 MET25-FLAG3:Sur4-F262A/K266L		-TRP-LEU-URA
SUR4# + CER3+CYTB5-B	pYES3GW	pESCLeu:GAL10:CER3-GAL1:CYTB5-B	p416 MET25-FLAG3:Sur4-F262A/K266L		-TRP-LEU-URA
SUR4# + CER1+CER3+CYTB5-B	pYES3GW:CER1	pESCLeu:GAL10:CER3-GAL1:CYTB5-B	p416 MET25-FLAG3:Sur4-F262A/K266L		-TRP-LEU-URA
SUR4# + CER1H146A+CER3+CYTB5-B	pESCTrp:GAL1:CER1H146A	pESCLeu:GAL10:CER3-GAL1:CYTB5-B	p416 MET25-FLAG3:Sur4-F262A/K266L		-TRP-LEU-URA
SUR4# + CER1H159A+CER3+CYTB5-B	pESCTrp:GAL1:CER1H159A	pESCLeu:GAL10:CER3-GAL1:CYTB5-B	p416 MET25-FLAG3:Sur4-F262A/K266L		-TRP-LEU-URA
SUR4# + CER1H248A+CER3+CYTB5-B	pESCTrp:GAL1:CER1H248A	pESCLeu:GAL10:CER3-GAL1:CYTB5-B	p416 MET25-FLAG3:Sur4-F262A/K266L		-TRP-LEU-URA
SUR4# + CER1+CER3H147A	pYES3GW:CER1	pESCLeu:GAL10:CER3H147A	p416 MET25-FLAG3:Sur4-F262A/K266L		-TRP-LEU-URA
SUR4# + CER1+CER3H161A	pYES3GW:CER1	pESCLeu:GAL10:CER3H161A	p416 MET25-FLAG3:Sur4-F262A/K266L		-TRP-LEU-URA
SUR4# + CER1+CER3H248A	pYES3GW:CER1	pESCLeu:GAL10:CER3H250A	p416 MET25-FLAG3:Sur4-F262A/K266L		-TRP-LEU-URA
SUR4#	pYES3GW	pESCLeu	p416 MET25-FLAG3:Sur4-F262A/K266L		-TRP-LEU-URA
SUR4# + CER1+CER3	pYES3GW:CER1	pESCLeu:GAL10:CER3	p416 MET25-FLAG3:Sur4-F262A/K266L	pESCHis	-TRP-LEU-URA-HIS
SUR4# + CER1+CER3+LACS1	pYES3GW:CER1	pESCLeu:GAL10:CER3	p416 MET25-FLAG3:Sur4-F262A/K266L	pESCHis:LACS1	-TRP-LEU-URA-HIS
SUR4# + CER1+CER3+CYTB5-B+LACS1	pYES3GW:CER1	pESCLeu:GAL10:CER3-GAL1:CYTB5-B	p416 MET25-FLAG3:Sur4-F262A/K266L	pESCHis:LACS1	-TRP-LEU-URA-HIS
SUR4# + LACS1	pYES3GW	pESCLeu	p416 MET25-FLAG3:Sur4-F262A/K266L	pESCHis:LACS1	-TRP-LEU-URA-HIS
SUR4#	pYES3GW	pESCLeu	p416 MET25-FLAG3:Sur4-F262A/K266L	pESCHis	-TRP-LEU-URA-HIS

Reconstitution of Plant Alkane Biosynthesis in Yeast Demonstrates That *Arabidopsis* ECERIFERUM1 and ECERIFERUM3 Are Core Components of a Very-Long-Chain Alkane Synthesis Complex

Amélie Bernard, Frédéric Domergue, Stéphanie Pascal, Reinhard Jetter, Charlotte Renne, Jean-Denis Faure, Richard P. Haslam, Johnathan A. Napier, René Lessire and Jérôme Joubès

Plant Cell 2012;24;3106-3118; originally published online July 6, 2012;
DOI 10.1105/tpc.112.099796